PHYSICS OF FLUIDS **26**, 052105 (2014)

Origin of ejecta in the water impact problem

R. Krechetnikov[a)]
Mechanical Engineering, University of California, Santa Barbara, California 93106, USA

(Received 12 November 2013; accepted 11 April 2014; published online 30 May 2014)

This work presents the analysis of the flow resulting from the flat plate impact on the surface of an incompressible viscous liquid at zero deadrise angle—of particular interest is the flow structure near the plate edge, $r \to 0$, evolving at early times, $t \to 0$. The deduced mathematical formulation proves to be of a singular perturbation type with the underlying governing equations having a linear structure. The key goals here are to elucidate the effects of viscosity and surface tension, which turn out to contribute to the solution at the leading order, and to resolve both $t \to 0$ and $r \to 0$ limit singularities in the classical pressure-impulse theory. In the course of construction of the solution, first the standard assumptions behind the existence of the inviscid approximation are revisited, which leads to correcting the previously known interpretation of the self-similarity of the classical inviscid solution near the plate edge. Second, new scalings of the solution structure near the plate edge are determined, with which the viscous solution near the edge is constructed analytically and matched to the inviscid one. Finally, the analysis of both the Stokes and inviscid limits of this uniformly valid solution allows us to uncover the scalings for the early time-evolution of ejecta—a jet forming during the impact—as well as to clarify the applicability of the Kutta-Joukowsky condition used in previous studies. [http://dx.doi.org/10.1063/1.4878843]

I. INTRODUCTION

The water impact problem has a long history[1,2] and goes back to a number of seminal studies which shaped the current theory. First, it is worth mentioning the studies by Joukowsky on the impact between two spheres, one of which is half submerged in liquid,[3] and of sea plane landing in 1898 also by Joukowsky[4] as well as by von Karman.[5] Later, Wagner[6] developed irrotational inviscid flow models for the impact loads and dynamics, and Sedov[7,8] laid out the impact theory in its classical form where motions with discontinuous changes in the velocity field are considered. Motivation for the problem also came from its relevance to other applications such as slamming of ships[9,10] to characterize structural and dynamic responses and impact of water waves on coastal structures.[11,12] One of the key aspects of the water impact problem is the formation of *ejecta*—the upward directed ejected liquid. In general, being formed during the very early times of the impact, when the highest force loads are experienced, and having much higher velocity than that of the impacting solid, the ejecta represents a fundamentally interesting phenomenon since it appears as a singularity caused by the sudden impact in time and sudden change in space in the boundary conditions from no-slip at the solid to no-shear at the free surface, cf. Figure 1. From a practical point of view, the ejecta is responsible for the fluid splash during the impact, which is sometimes an unwanted phenomenon in various applications.

While ejecta arises in many other impact problems, e.g., impact of solids of other shapes,[13,14] liquid drops,[15] impact on liquid bodies of varying depth,[16,17] for the sake of precision and because of the direct relevance to the present study, below we will mention only the works concerning the impact of a flat plate (disk) on deep water at zero deadrise angle. On the experimental side, the

[a)]Present address: Mathematical and Statistical Sciences, University of Alberta, Edmonton, Alberta T6G 2G1, Canada.

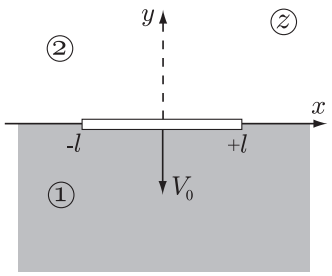

FIG. 1. Plate impact problem.

problem received wide attention.[13,17–19] On the theoretical side, the problem was studied by both analytical and numerical[20] means. But, as noted by Korobkin,[21] because of the complexity of the liquid-solid impact phenomenon all available theoretical models of the impact are limited in their validity, with limitations of numerical models being much stronger than that of theory. Therefore, analytical models are indispensable in predicting the evolution of the impact process. Historically, the problem of a plate impact on water surface was tackled with conformal mapping techniques[14,22] and asymptotic methods[21] for both incompressible[22,23] and compressible[24–26] liquids, to mention a few.

These previous studies formed the following view on the formation of ejecta. To make the discussion specific, let us follow the classical formulation[27] shown in Figure 1 and consider the two-dimensional problem of the impact of an infinitely thin plate of width $2\,l$ and mass m on the interface between a semi-infinite body of a quiescent incompressible fluid 1 of density ρ_0 and inertialess and inviscid phase 2; the latter condition allows one to avoid the air-cushion effect—air trapped between the plate and the fluid surface, which has been studied extensively.[18,28,29] Since in this work we are interested in the flow structure, but not the loads, without loss we will assume that $m = \infty$, which entails that the speed of the plate does not change between before and after the impact event at $t = 0$, $V_{-0} = V_{+0} \equiv V_0$. As formally argued in the classical texts,[22,23,27,30] based on physical considerations, if the question is to predict the fluid velocity distribution right after the impact moment, $t = +0$, then the fluid viscosity and vorticity[31] can be neglected. Indeed, if there are no mass impulsive forces, then neither convective nor viscous terms can balance the dominant time-derivative, $\partial\mathbf{v}/\partial t$, but only the sudden pressure gradients can balance this change in fluid motion:

$$\frac{\partial \mathbf{v}}{\partial t} = -\frac{1}{\rho}\nabla p. \tag{1}$$

Then the fluid incompressibility, $\nabla\mathbf{v} = 0$, implies that the pressure p is a harmonic function, $\Delta p = 0$, and thus the fluid motion is potential right after the impact with $\mathbf{v} = \nabla\phi$, where ϕ is the usual velocity potential, also a harmonic function, $\Delta\phi = 0$. To establish a relation between pressure p and velocity potential ϕ, one can integrate the momentum equation (1) to produce

$$\phi|_{t=+0} - \phi|_{t=-0} = -\frac{1}{\rho}\Pi, \text{ where } \Pi \equiv \int_{-0}^{+0} p\,\mathrm{d}t, \tag{2}$$

which yields the expression for the impulsive pressure $\Pi = -\rho\,\phi|_{t=+0}$ since there is no initial non-trivial flow field, $\phi|_{t=-0} = 0$, prior to the impact. The impulsive nature of the problem is reflected in the fact that the time-dependence of the solution of (1) for $t \to 0$ is $\mathbf{v}(\mathbf{x}, t) \sim H(t)$ and hence $p(\mathbf{x}, t) \sim \delta_D(t)$, where $H(t)$ is the Heaviside step function and $\delta_D(t)$ the Dirac delta-function with $\dim = T^{-1}$. This is the basis of the classical pressure-impulse theory.

Thus, for $t \to 0$, one can consider the water impact as the boundary value problem in the inviscid potential flow approximation with the boundary conditions at $y = 0$:

$$\text{solid plate, } x \in [-l, l]: \ \frac{\partial\phi}{\partial y} = -V_0, \tag{3a}$$

$$\text{free interface, } x \notin [-l, l]: \ \phi = 0. \tag{3b}$$

The corresponding two-dimensional solution can be constructed with conformal mapping techniques[22,23] for the complex velocity potential $f(z) = \phi(z) + i\psi(z)$:

$$f(z) = iV_0\left(z - \sqrt{z^2 - l^2}\right), \tag{4}$$

with $z = x + iy$ being the independent variable in the two-dimensional plane. This solution has a singularity at the plate edge with both velocity components $u - iv = f'(z)$ blowing up at time $t = +0$ in the vicinity of the plate edge,

$$\mathbf{v} \sim r^{-1/2}, \tag{5}$$

where r is the radius coordinate positioned at the plate edge. Yakimov[19] was the first to study the local behavior of the free interface close to the edge of a plate entering water with the aim of understanding the effect of the atmosphere density on the geometry of the jet generated by the impact. By using simple dimensional consideration of the scaling (5) for the velocity near the edge, he argued that during the initial stage the local flow is self-similar in the time-stretched variables $(r, \theta) \to (rt^{-2/3}, \theta)$, where (r, θ) are the polar coordinates with the origin at the plate edge. These self-similar variables introduced by Yakimov were adopted in a number of other studies[32–34] and tested at the free interface versus potential flow numerical simulations[35,36] and experimental data,[19,32,34] but not in the bulk (e.g., by comparing with the velocity field) as will be discussed in detail in Sec. VI A. Also, in the inviscid approximation studies,[32,35–37] an additional constraint—the Kutta-Joukowsky condition—was enforced at the plate edge requiring that the free surface is tangentially attached to the plate edge.

Despite all these previous efforts, the singularity (5) of the inviscid potential approximation leaves the question on how to resolve it based on true physics, which is the focus of the present study. In analogy with the boundary layer separation from the trailing edge,[38,39] it is natural to expect that viscosity ν should play a role, and from the fact that we have a free interface, interfacial energy needs to be taken into account through incorporating surface tension σ. These two facts can be seen from the definitions of the Reynolds $Re = V_0 r/\nu$ and Weber $We = \rho V_0^2 r/\sigma$ numbers, which reflect on the competition at some spatial scale r between inertia versus viscous and surface tension effects, respectively. Clearly, there exists a distance r from the edge defining the scales on which these numbers become $O(1)$, thus indicating the importance of viscous and surface tension forces. By resolving the physics directly, we can develop viscous and inviscid scalings for the early time-evolution of the ejecta and thus naturally address the question of applicability of the Kutta-Joukowsky condition near the edge plate, which is necessary in the inviscid approximation similar to the airfoil theory.[40]

The outline of the paper is as follows. First, following the above discussion, in Sec. II we formulate the problem, which sets limits of applicability of the present study. In Sec. III, we recall the near-the-edge asymptotics, which allows us to arrive in Sec. IV at the new self-similar scaling valid in both viscous and inviscid cases and thus enabling us to build a solution uniformly valid in both viscous and inviscid regions (Sec. V) and then analyze the interface dynamics (Sec. VI).

II. PROBLEM FORMULATION

In view of the geometry of the physical system introduced in the Introduction and shown in Figure 1, it is convenient to treat the problem near the edge in polar coordinates, cf. Figure 2. The bulk dynamics governed by the Navier-Stokes equations (NSEs) for incompressible fluid, however, proves to be more concise to consider first in the Cartesian (x, y)-coordinates (as will be done in Sec. IV):

$$\frac{\partial u}{\partial x} + \frac{\partial v}{\partial y} = 0, \tag{6a}$$

$$Lu = -\frac{1}{\rho}\frac{\partial p}{\partial x} + \nu\Delta u, \tag{6b}$$

$$Lv = -\frac{1}{\rho}\frac{\partial p}{\partial y} + \nu\Delta v - g, \tag{6c}$$

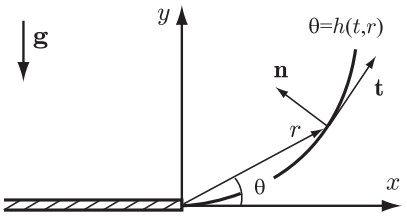

FIG. 2. Near the plate edge region.

where $L = \partial_t + u\partial_x + v\partial_y$ is the advection operator and g the gravitational acceleration.

While the boundary conditions at the plate surface are the standard no-slip and no-penetration,

$$u = 0, \ v = -V_0, \tag{7}$$

respectively, the fluid interface in the gravity field $\mathbf{g}$, cf. Figure 2, requires special consideration, naturally in polar coordinates, $\theta = h(t, r)$. The dynamic condition at the interface can be decomposed into components that are tangential along the vector $\mathbf{t}$ and normal along the vector $\mathbf{n}$ pointing out of the fluid phase:

$$\mathbf{t} \cdot \mathbf{T} \cdot \mathbf{n} = \mathbf{t} \cdot \nabla_s \sigma, \tag{8a}$$

$$-\mathbf{n} \cdot \mathbf{T} \cdot \mathbf{n} = \sigma \, \nabla \cdot \mathbf{n}, \tag{8b}$$

respectively. Here $\nabla_s = \mathbf{t} \cdot \nabla$ the interfacial gradient and $\mathbf{T}$ the stress tensor with the components[41]

$$T_{rr} = -p + 2\,\mu\, u_r, \ T_{r\theta} = \mu\left(\frac{1}{r}u_\theta + v_r - \frac{v}{r}\right), \ T_{\theta\theta} = -p + 2\,\mu\left(\frac{1}{r}v_\theta + \frac{u}{r}\right),$$

where u and v are the r- and θ-components of the velocity vector, respectively (for brevity, we do not introduce new notations for the velocity components in polar coordinates), $\mu = \rho\,\nu$ is the dynamic viscosity, and the subscripts stand for the derivatives with respect to the corresponding coordinates.

In what follows, we will treat the case when surface tension σ is constant, i.e., we do not account for the rheology of surface tension and possible associated transport. If the normal and tangential vectors in polar coordinates $(\boldsymbol{r}, \boldsymbol{\theta})$ are defined by

$$\mathbf{n} = \frac{\nabla H}{|\nabla H|} = \frac{-\boldsymbol{r} h_r + \boldsymbol{\theta}\frac{1}{r}}{\sqrt{r^{-2} + h_r^2}}, \ \mathbf{t} = \frac{\boldsymbol{r}\frac{1}{r} + \boldsymbol{\theta} h_r}{\sqrt{r^{-2} + h_r^2}}, \tag{9}$$

respectively, then both pairs $(\boldsymbol{r}, \boldsymbol{\theta})$ and $(\mathbf{t}, \mathbf{n})$ are right-handed coordinate systems. The curvature is

$$\nabla \cdot \mathbf{n}|_{\theta = h(t,r)} = -\frac{1}{r}\frac{1}{(1 + r^2 h_r^2)^{3/2}}\left[2\,r\,h_r + r^2 h_{rr} + r^3 h_r^3\right], \tag{10}$$

and in the limit $r \to 0$, $\nabla \cdot \mathbf{n} \simeq -2\,h_r - r h_{rr}$ under the appropriate assumptions on the smallness of $r\,h_r$ as $r \to 0$, which will be verified a posteriori once the solution for the ejecta shape is constructed in Sec. VI. Finally, the system is closed with the kinematic condition, which can be written using an implicit representation of the interface, $H = \theta - h(t, r)$:

$$\frac{\partial H}{\partial t} + \nabla H \cdot \mathbf{v} = 0, \ \text{so that} \ \frac{\partial h}{\partial t} + u\frac{\partial h}{\partial r} = \frac{v}{r} \ \text{at} \ \theta = h(t, r), \tag{11}$$

which is the vanishing total (material) derivative, and in physical terms implies that velocity of the liquid normal to the interface, $\nabla H \cdot \mathbf{v}/|\nabla H|$, should be equal to that of the interface, $H_t/|\nabla H|$, for the sake of the fluid continuity.

And, finally, since we are interested only in the early time-evolution, from now on we will consider the leading order dynamic (8) and kinematic (11) boundary conditions at the interface, $\theta = h(t, r)$. Assuming, for concreteness, perfect wetting of an infinitely thin plate, small departures

$h(t, r)$ from $\theta = 0$ at short times, and $r\,h_r \ll 1$ as $r \to 0$, we get

$$-p + \frac{2\mu}{r}\,(v_\theta + u) = \sigma\ [2\,h_r + r h_{rr}]\,, \tag{12a}$$

$$\mu\left(v_r - \frac{v}{r} + \frac{1}{r}u_\theta\right) = 0, \tag{12b}$$

$$h_t + u h_r = \frac{v}{r}, \tag{12c}$$

where for the purpose of the subsequent discussion, we retain the only "nonlinear" term $u\,h_r$ in the kinematic boundary condition.[42]

III. NEAR-THE-EDGE INVISCID SOLUTION ASYMPTOTICS

Since we are analyzing the formation of ejecta due to the singularity near the plate edge, let the plate fall onto the negative semi-axis, $x' \in \mathbb{R}^-$. Then, the complex potential near that edge can be obtained from (4) by shifting the coordinate system, $x \to x' + l$ $(z \to z' + l)$,

$$f(z') \simeq -i\,\alpha\sqrt{2\,z'}, \tag{13}$$

where we retained the leading order non-constant term only[43] and $\alpha = V_0\sqrt{l}$ with $\dim\alpha = L^{3/2}T^{-1}$. Notably, (13) is analogous to the solution for a flow around a sharp corner of zero angle.[41]

Separating real and imaginary parts of the complex velocity potential (13), we get the dimensional stream-function

$$\psi = -\alpha\sqrt{2\,r}\cos\frac{\theta}{2}, \tag{14}$$

which yields the shape of a given streamline $\psi = \text{const}$, $r(\theta) = \psi^2/[2\alpha^2\cos^2(\theta/2)]$, with $r_\theta \le 0$ and $r_{\theta\theta} \ge 0$ for any $-\pi \le \theta \le 0$ – the instantaneous flow field corresponding to $t = 0$ is shown in Figure 3(a). Calculation of the x' and y velocity components from Eq. (14),

$$\mathbf{v}_0(x', y):\ u = -\frac{\alpha}{\sqrt{2\,r}}\sin\frac{\theta}{2},\ v = \frac{\alpha}{\sqrt{2\,r}}\cos\frac{\theta}{2}, \tag{15}$$

gives the following conditions at the plate surface, $\theta = -\pi$, and the interface, $\theta = 0$,

$$\theta = -\pi : u = \frac{\alpha}{\sqrt{2\,r}},\ v = 0, \tag{16a}$$

$$\theta = 0 : u = 0,\ v = \frac{\alpha}{\sqrt{2\,r}}, \tag{16b}$$

respectively. The intuition behind this solution and thus the origin of ejecta is that once the plate impacts the surface, a layer of displaced liquid beneath it moves radially and since it fails to accelerate the bulk of surrounding liquid, this layer is deflected upwards and forms an ejecta. One can easily verify that the irrotational character of the flow is preserved in this approximation. Note that $v = 0$

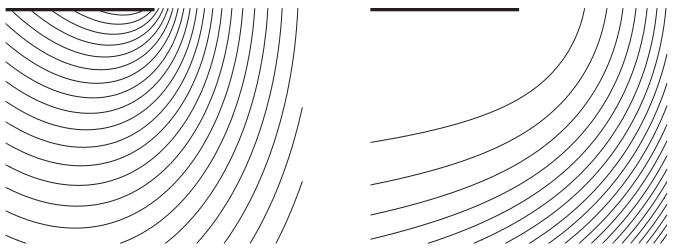

(a) (b)

FIG. 3. Inviscid (a) and viscous (b) streamline patterns near the plate edge, as given by equations (14) and (38), respectively.

at the plate surface in this approximation as opposed to (7) because we retain the leading order term only when arriving at (13), so in the subsequent analysis the conditions (7) are substituted by

$$\theta = -\pi : \ u = 0, \ v = 0. \tag{17}$$

The true value, of course, should be $v = -V_0$, which means that next order corrections to (15) are not self-similar.

Finally, integrating (1) one can determine the impulsive pressure Π asymptotics near the plate edge:

$$\Pi \equiv \int_{-0}^{+0} p \, \mathrm{d}t = -\rho \, \phi|_{t=+0} = -\rho \, \alpha \sqrt{2r} \sin \frac{\theta}{2}, \tag{18}$$

that is the pressure is given by

$$p(t, r, \theta) = -\rho \, \alpha \sqrt{2r} \sin \frac{\theta}{2} \, \delta_D(t). \tag{19}$$

The apparent limitations of the above near the edge asymptotics (5,15) consist in the singularity of the self-similar solution, which entails unbounded values of the velocity field. In particular, the infinite vertical velocity component implies that the interface will become infinitely extended, which is non-physical as the interface should have a finite energy (surface tension) since a finite energy is transferred to the fluid. Indeed, despite the infinite mass of the impacting plate assumed here (cf. the Introduction) it is straightforward to show that the energy acquired by the fluid is finite and based on (4) decays with the distance from the origin as r^{-4}—this fact is at the basis of the fundamental concept of added mass.[23] Therefore, even though some parts of the fluid near the plate edges have an infinite speed, their contribution to the overall energy is infinitesimally small. However, the interface of an infinite extent and finite surface tension σ cannot be neglected in the overall energy balance. Thus, the key question is how to resolve the singularity (5) and to provide the interpretation for this self-similar solution from the time-evolution point of view.

IV. SCALING

As pointed out in the Introduction, the singularity (5,15) should be resolved with the viscosity and surface tension effects. First, the viscosity comes into play because the no-slip boundary condition at the plate surface should be satisfied, which leads to the formation of the boundary layer as discussed in Appendix A. Second, as mentioned at the end of the previous section, the singular velocity distribution (15) implies that the fluid interface acquires an infinite area, which is impossible energetically if surface tension is taken into account as an interface of infinite extent would have infinite energy. Hence, the key conclusion is that surface tension and viscosity must have an effect immediately after impact.

The idea here is not only to demonstrate the validity of this conclusion, but to develop a view on the phenomena taking into account the continuity of the solution for $t \geq 0$, which in the limit $t = +0$ should recover the classical potential flow solution (4). Let us start with the Yakimov scaling suggested by (5) based solely on the dimensionality considerations and used in this form in other works,[32–36] i.e.,

$$\mathbf{v} \sim \frac{\mathrm{d}\boldsymbol{r}}{\mathrm{d}t} \sim \frac{\alpha}{\sqrt{|\boldsymbol{r}|}}, \ \text{so that } (x, y) = \alpha^{2/3} t^{2/3} (\widetilde{x}, \widetilde{y}) \text{ and } \mathbf{v} = t^{-1/3} \widetilde{\mathbf{v}}(\widetilde{x}, \widetilde{y}), \tag{20}$$

which means that "everything interesting" happens for $|\boldsymbol{r}| \sim O(t^{2/3})$; pressure then would scale as $p = \rho \, \alpha^{4/3} t^{-2/3} \widetilde{p}$ to balance $\partial \mathbf{v}/\partial t$ as required in the pressure-impulse theory argument.[22] As easy to show, with this choice nonlinear advection terms are of the same order as the time-derivative term,

$$L\mathbf{v} \sim (\mathbf{v} \cdot \nabla) \, \mathbf{v} \sim \partial \mathbf{v}/\partial t \sim \alpha^{2/3} t^{-4/3}, \tag{21}$$

while viscous terms after rescaling acquire the following effective Reynolds number:

$$Re = \alpha^{4/3} t^{1/3} \, \nu^{-1}, \tag{22}$$

that is for $t \lesssim \nu^3\alpha^{-4}$ viscous terms would be important (i.e., $Re \lesssim 1$) if one uses Yakimov's anzatz (20). Therefore, the scaling (20) is not appropriate for studying the limit $t \to 0$ once viscosity is taken into account since with this scaling one cannot justify the inviscid solution (4) discussed in the Introduction and Sec. III[44]—as $t \to +0$ the solution would not approach the inviscid one because based on (22) viscous effects would become increasingly important for short times. In this context, it is also important to point out that the assertion that "in the limit $t \to 0$ one must recover the inviscid potential solution" is to be preserved after a self-similar scaling is applied to equations since self-similarity simply limits the possible solutions of the corresponding partial differential equations to a more narrow class. The scaling (20) is flawed in this sense as demonstrated above.

Thus, the correct self-similar scaling should be based on the fact that the inviscid solution is valid in some sense for $t = 0$, viscosity is important for $t > 0$ immediately after the impact because the no-slip boundary condition on the plate should be satisfied at any time, and $\mathbf{v} \sim \alpha\,|\boldsymbol{r}|^{-1/2}$ to conform with the inviscid solution, cf. (5,15). This reasoning leads to (from now on we will use notations with the tilde for the transformed non-dimensional variables)

$$t \to \frac{l}{V_0}\tau,\ (x, y) \to \beta\, t^{\gamma}(\widetilde{x}, \widetilde{y}),\ \mathbf{v} \to \frac{\alpha}{\beta^{1/2}t^{\gamma/2}}\widetilde{\mathbf{v}}(\widetilde{x}, \widetilde{y}),\ \ p \to \rho\,\alpha\,\beta^{1/2}t^{\gamma/2-1}\widetilde{p}, \tag{23}$$

where α was defined in (13) and the constant β along with the power γ are to be determined from the balance of (forces) terms in the NSEs (6), e.g., in the x-component of the momentum equation:

$$\begin{aligned} -\frac{\gamma}{2}\widetilde{u} - \gamma\left(\widetilde{x}\,\widetilde{u}_{\widetilde{x}} + \widetilde{y}\,\widetilde{u}_{\widetilde{y}}\right) + \left(\frac{V_0}{l}\right)^{\frac{3}{2}\gamma-1}\frac{\alpha}{\beta^{3/2}}\tau^{1-\frac{3\gamma}{2}}\left(\widetilde{u}\,\widetilde{u}_{\widetilde{x}} + \widetilde{v}\,\widetilde{u}_{\widetilde{y}}\right) = \\ -\widetilde{p}_{\widetilde{x}} + \nu\left(\frac{V_0}{l}\right)^{2\gamma-1}\frac{\tau^{1-2\gamma}}{\beta^2}\left(\widetilde{u}_{\widetilde{x}\widetilde{x}} + \widetilde{u}_{\widetilde{y}\widetilde{y}}\right), \end{aligned} \tag{24}$$

and similarly for the y-component. Note that the general scaling (23) admits the value $\gamma = 2/3$ as in (20). However, in order to arrive at the inviscid potential solution in the limit $\tau \to 0$ one needs nonlinear inertia to be negligible for small times, $\tau \ll 1$, which leads to the first condition $1 - 3\gamma/2 > 0$—the question as to when nonlinear intertia becomes important will be addressed in Sec. V. The second condition says that viscous terms should be also non-dominating, which requires $1 - 2\gamma \geq 0$. Altogether, this imposes $\gamma \leq 1/2$. However, the no-slip boundary condition should be satisfied at all times, which brings us to balancing inertia and viscous terms thus leading to $\gamma = 1/2$ (note that pressure is already balanced with inertia), while β must be equal to $\sqrt{V_0\,l}$, since the coefficients in front of nonlinear and viscous terms should be non-dimensional. The determined value of the exponent γ sets the coordinate scaling corresponding to the rate at which viscous effects diffuse away from the plate and also makes sense as it matches the boundary layer growth below the plate, cf. Appendix A.

With these values of γ and β, Eq. (24) is simplified to (and similarly for the y-component of the momentum equation):

$$-\frac{1}{4}\widetilde{u} - \frac{1}{2}\left(\widetilde{x}\,\widetilde{u}_{\widetilde{x}} + \widetilde{y}\,\widetilde{u}_{\widetilde{y}}\right) + \tau^{1/4}\left(\widetilde{u}\,\widetilde{u}_{\widetilde{x}} + \widetilde{v}\,\widetilde{u}_{\widetilde{y}}\right) = -\widetilde{p}_{\widetilde{x}} + \frac{1}{Re_0}\left(\widetilde{u}_{\widetilde{x}\widetilde{x}} + \widetilde{u}_{\widetilde{y}\widetilde{y}}\right), \tag{25}$$

where $Re_0 = V_0\,l/\nu$. From here we can conclude that the nonlinear inertia terms are negligible compared to the viscous terms when $\tau^{1/4} \ll Re_0^{-1}$, i.e., for short time we are interested in the present analysis. The resulting non-dimensional system at the leading order becomes linear[45]

$$\widetilde{u}_{\widetilde{x}} + \widetilde{v}_{\widetilde{y}} = 0, \tag{26a}$$

$$-\frac{1}{4}\widetilde{u} - \frac{1}{2}\left(\widetilde{x}\,\widetilde{u}_{\widetilde{x}} + \widetilde{y}\,\widetilde{u}_{\widetilde{y}}\right) = -\widetilde{p}_{\widetilde{x}} + \frac{1}{Re_0}\left(\widetilde{u}_{\widetilde{x}\widetilde{x}} + \widetilde{u}_{\widetilde{y}\widetilde{y}}\right), \tag{26b}$$

$$-\frac{1}{4}\widetilde{v} - \frac{1}{2}\left(\widetilde{x}\,\widetilde{v}_{\widetilde{x}} + \widetilde{y}\,\widetilde{v}_{\widetilde{y}}\right) = -\widetilde{p}_{\widetilde{y}} + \frac{1}{Re_0}\left(\widetilde{v}_{\widetilde{x}\widetilde{x}} + \widetilde{v}_{\widetilde{y}\widetilde{y}}\right) - \frac{1}{Fr}\,\tau^{5/4}, \tag{26c}$$

where $Fr = V_0^2/(g\,l)$ is the Froude number. Note that the gravity term is negligible for small times, $\tau \ll 1$, as long as $\tau^{5/4}/Fr \ll 1$. The viscosity is important on the scales $(\widetilde{x}, \widetilde{y}) \lesssim O(Re_0^{-1/2})$, i.e., in

physical variables, as argued in Appendix A, this is true only near the edge over the distances of the order of $\sqrt{\nu\, t}$, which is the boundary layer thickness. Outside the boundary layer, the solution can be treated in the inviscid approximation. In what follows, we will consider both viscous and inviscid approximations.

Introduction of polar coordinates, $\widetilde{x} = \widetilde{r}\,\cos\theta$ and $\widetilde{y} = \widetilde{r}\,\sin\theta$, a stream-function $\widetilde{\psi}$, such that $\widetilde{u} = \widetilde{\psi}_{\widetilde{y}}$ and $\widetilde{v} = -\widetilde{\psi}_{\widetilde{x}}$, and the function $f = \Delta\widetilde{\psi}$ reduces (26) to

$$\frac{3}{2} f + \widetilde{r}\, f_{\widetilde{r}} + \varepsilon\, \Delta f = 0, \tag{27a}$$

$$f = \Delta\widetilde{\psi}, \tag{27b}$$

where $\varepsilon = 2/Re_0$, the function f has the meaning of the vorticity with minus sign, and Eq. (27) should satisfy the no-slip boundary condition

$$\theta = -\pi : \ \widetilde{\psi} = \widetilde{\psi}_\theta = 0, \tag{28}$$

along with the dynamic and kinematic conditions at the interface, $\theta = 0$, discussed below. For convenience, we also introduce velocity components in polar coordinates defined by

$$\widetilde{u} = \frac{1}{\widetilde{r}}\frac{\partial\widetilde{\psi}}{\partial\theta}, \ \widetilde{v} = -\frac{\partial\widetilde{\psi}}{\partial\widetilde{r}}, \tag{29}$$

with $(\widetilde{u}, \widetilde{v})$ now standing for the $(\boldsymbol{r}, \boldsymbol{\theta})$-velocity components, respectively. Finally, the pressure $\widetilde{p}$ turns out to be determined by the Laplace equation,

$$\Delta\widetilde{p} = 0. \tag{30}$$

Although above we were able to identify the scaling (23), which justifies the impulsive inviscid limit discussed in the Introduction and brings the viscous terms to the leading order, we have not taken the free boundary conditions into consideration. Let us also apply (23) to the leading order boundary conditions (12) at the interface, $\theta = 0$, to find

$$-\widetilde{p} + \frac{\varepsilon}{\widetilde{r}}\left(\frac{1}{\widetilde{r}}\widetilde{\psi}_\theta - \widetilde{\psi}_{\widetilde{r}\theta}\right) = \frac{\tau^{1/4}}{We}\left[2\, h_{\widetilde{r}} + \widetilde{r}\, h_{\widetilde{r}\widetilde{r}}\right], \tag{31a}$$

$$\frac{\varepsilon}{\tau^{3/4}}\left(\frac{1}{\widetilde{r}^2}\widetilde{\psi}_{\theta\theta} + \frac{1}{\widetilde{r}}\widetilde{\psi}_{\widetilde{r}} - \widetilde{\psi}_{\widetilde{r}\widetilde{r}}\right) = 0, \tag{31b}$$

$$h_\tau - \frac{1}{2}\frac{\widetilde{r}}{\tau}\, h_{\widetilde{r}} = -\frac{1}{\tau^{3/4}}\frac{1}{\widetilde{r}}\left[\widetilde{\psi}_{\widetilde{r}} + h_{\widetilde{r}}\widetilde{\psi}_\theta\right], \tag{31c}$$

where $We = \rho\, V_0^2\, l/\sigma$ is the Weber number measuring importance of the surface tension forces relative to inertia.

V. VISCOUS SELF-SIMILAR SOLUTION

In view of the linearity of the problem defined by (27) with the boundary conditions ((17), (31)), as will be shown below we will be able to construct first the velocity field satisfying (17) and (31b), and then the pressure field (30) with the boundary condition (31a), and finally the ejecta evolution from (31c).

Let us first construct the velocity field obeying (27) and ((17), (31b)), which can be matched to the inviscid solution. The viscous solution should satisfy the sudden change in the boundary condition from the no-slip on the plate surface to the no-shear at the free boundary. This is analogous to the leading[46–48] and trailing[49,50] edge solutions for a flow around a flat plate, but the key difference here is that for short times the solution is governed by a linear system of equations, i.e., nonlinear advection terms are negligible.

A. Solution

The general solution to (27) uniformly valid in both viscous and inviscid regions can be constructed using separation of variables, cf. Appendix B, and represents a sum of a general solution $\widetilde{\psi}_p(\widetilde{r},\theta)$ of the inhomogeneous part of the problem (27b) and a general solution $\widetilde{\psi}_h(\widetilde{r},\theta)$ of the homogeneous (harmonic) part of the Poisson equation (27b) in polar coordinates:

$$\begin{aligned}\widetilde{\psi}(\widetilde{r},\theta)=\widetilde{\psi}_p+\widetilde{\psi}_h=&\sum_{m=0}^{\infty}\left(A_m\cos\beta_m\theta+B_m\sin\beta_m\theta\right)R_m(\widetilde{r})\\&+\sum_{n=-\infty}^{+\infty}\widetilde{r}^{\,n+\frac{1}{2}}\left\{C_n\cos\left(n+\tfrac{1}{2}\right)\theta+D_n\sin\left(n+\tfrac{1}{2}\right)\theta\right\},\end{aligned}\tag{32}$$

where $R_m(\widetilde{r})=\widetilde{r}^{\,\beta_m+2}H_m(\zeta)$ and special function $H_m(\zeta)=H(\zeta,\beta_m)$ given by (B14) corresponds to the value $\beta_m=\beta_0+m$, $\beta_0=1/2$.

Since the solution (32) does not have the simple structure $\sim\widetilde{r}^{\,n}\,\Theta_n(\theta)$, as $R_m(\widetilde{r})$ is a general function of $\widetilde{r}$ as opposed to the polynomial form $\widetilde{r}^{\,n}$ (as in the inviscid and Stokes regions) in the solution $\widetilde{\psi}_h$ of the homogeneous part of (27b), we cannot satisfy the three boundary conditions (28) and (31b) for each factor of $R_m(\widetilde{r})$ or that of $\widetilde{r}^{\,n}$ in the solution (32). However, since the confluent hypergeometric functions of the first kind can be represented in power series:[51]

$$M(\widehat{a},\widehat{b},\zeta)=\sum_{n=0}^{\infty}\frac{(\widehat{a})_n}{(\widehat{b})_n}\frac{\zeta^n}{n!},\ \text{where}\ (\widehat{a})_n=\widehat{a}\,(\widehat{a}+1)\ldots(\widehat{a}+n-1),\ (\widehat{a})_0=1,\tag{33}$$

(and similarly for $(\widehat{b})_n$) along with its integrals in (B14), the general solution (32) of (27) can be rewritten in the power-law form

$$\begin{aligned}\widetilde{\psi}(\widetilde{r},\theta)=&\sum_{m=0}^{\infty}\left\{\left(A_m\cos\beta_m\theta+B_m\sin\beta_m\theta\right)\widetilde{r}^{\,\beta_m+2}\sum_{n=0}^{\infty}\widetilde{c}_{mn}\widetilde{r}^{\,2n}\right\}\\&+\sum_{s=2}^{\infty}\widetilde{r}^{\,\beta_s}(C_s\cos\beta_s\theta+D_s\sin\beta_s\theta),\end{aligned}\tag{34}$$

where $\beta_m=\beta_0+m$ and same for β_s, and coefficients $\widetilde{c}_{mn}$ are known from (33) and integrals of $M(\widehat{a},\widehat{b},\zeta)$ in (B14). This form of the solution makes it possible to satisfy the boundary conditions (28) and (31b) for each function $\Theta_p(\theta)$ corresponding to $\widetilde{r}^{\,p}$:

$$\Theta_p(\theta)=C_p\cos\beta_p\theta+D_p\sin\beta_p\theta+\sum_{\substack{m,n=0\\2+\beta_m+2n=p}}^{\infty}\widetilde{c}_{mn}(A_m\cos\beta_m\theta+B_m\sin\beta_m\theta),\tag{35}$$

but requires that the solution (32) is in the form of an infinite series of polynomials. This procedure allows one to determine the constants in the infinite series (32), which satisfies the boundary conditions (28,31b) as follows from the power-law representation (34) of the same solution.

B. Inviscid and Stokes limits

Let us summarize the inviscid and Stokes limits of the solution (34). In the inviscid approximation, $\varepsilon=0$, i.e., when viscous terms in (27) are absent, it gives

$$\widetilde{\psi}(\widetilde{r},\theta)=A_0\,\widetilde{r}^{\,1/2}\cos\frac{\theta}{2},\tag{36}$$

which is consistent with the solution (14) found with the help of the complex variable analysis; comparison gives $A_0=-\sqrt{2}$, where we used the fact that $\psi=l\,V_0\,\tau^{1/4}\,\widetilde{\psi}$. Going back from $(\widetilde{x},\widetilde{y})$- to the physical (x,y)-plane, i.e., inverting the transformation (23), tells us that the leading order solution for short times, $\tau\ll1$, for the velocity field is time-independent (15). The pressure field is given by (19). It must be noted, however, that this inviscid limit of the solution for the velocity field

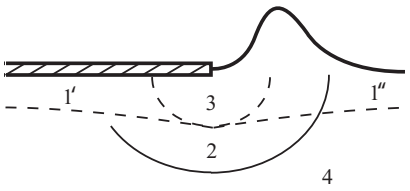

FIG. 4. Flow structure near the plate edge: region $1'$ is the wall jet (boundary layer), region $1''$ is the interfacial viscous sublayer, region 2 is inviscid self-similar $\widetilde{r} \gg \varepsilon^{1/2}$, region 3 is viscous self-similar $\widetilde{r} \sim \varepsilon^{1/2}$, and region 4 is the inviscid non-self-similar.

is the leading order one consistent with the classical inviscid (pressure-impulse) solution constructed via conformal mapping technique discussed in the Introduction.

In the Stokes subregion, $\widetilde{r} \ll \sqrt{\varepsilon}$, of the viscous region 3, cf. Figure 4, (27) reduces to

$$\Delta^2 \widetilde{\psi} = 0, \tag{37}$$

which can be arrived at by introducing a new rescaled radial coordinate $\widetilde{\rho} = \delta^{-1}\widetilde{r}$, $\delta \ll \varepsilon^{-1/2}$, but for the sake of simplicity of notation we will work with the original variable $\widetilde{r}$. The solution $\widetilde{\psi}(\widetilde{r}, \theta) = R(\widetilde{r})\,\Theta(\theta)$ of (37) proves to have $R(\widetilde{r})$ in the polynomial form. As follows from the discussion in Appendix B, the non-trivial Stokes solution of (37) satisfying (28,31b) with the lowest n corresponds to $n = 5/2$, which in general reads

$$\widetilde{\psi} = C^{(c)}\widetilde{r}^{5/2}\left[\cos\frac{5\theta}{2} - 5\cos\frac{\theta}{2}\right] + C^{(s)}\widetilde{r}^{5/2}\left[\sin\frac{5\theta}{2} - \sin\frac{\theta}{2}\right]. \tag{38}$$

Should this leading order Stokes solution be constructed independently without recourse to the uniformly valid viscous solution (34), it would contain undetermined constants. This is a common problem for elliptic equations,[52] for which coordinate expansions give only qualitative results—due to dependence on all boundary conditions, local solutions such as the above Stokes solution depend on boundary conditions at large distances. Therefore, the determined expansions contain unknown constants, which often cannot be found as they depend on the boundary conditions far from the region of applicability of the constructed solution. An analogous situation arises for the flow past a semi-infinite flat plate.[46,47,52] However, in our case these constants, $C^{(c)}$ and $C^{(s)}$, can be determined. In particular, since the "sine" part vanishes based on matching to the inviscid solution, $C^{(s)} = 0$, the solution is as shown in Figure 3(b) and should be compared to the inviscid flow around the edge in Figure 3(a) given by (14). Notably, this value of $n = 5/2$ is different from $n = 3/2$ obtained for the flow about the leading edge[46] and for the flow near the intersection of rigid and free surfaces.[53]

C. The structure of the solution

Given all the above formal considerations, which establish the existence of a solution to (27) with the boundary conditions (17,31b) let us focus on the key part of the solution (32) for $\widetilde{\psi}$, by taking into account the powers of $\widetilde{r}$ relevant to the inviscid and Stokes solutions

$$\widetilde{\psi}(\widetilde{r}, \theta) = R_0(\widetilde{r})\cos\frac{\theta}{2} + C^{(c)}\widetilde{r}^{\,5/2}\cos\frac{5\theta}{2}, \tag{39}$$

respectfully, from which we can recover the asymptotics for $\widetilde{r} \ll \varepsilon^{1/2}$ and $\widetilde{r} \gg \varepsilon^{1/2}$. In the Stokes region, for $\widetilde{r} \ll \varepsilon^{1/2}$, we get $H_0(\zeta) = C_1/6$ so that $R_0 = C_1\widetilde{r}^{5/2}/6$ and thus $C^{(c)} = -C_1/30$. And in the inviscid region, for $\widetilde{r} \gg \varepsilon^{1/2}$ ($\zeta \to -\infty$), we arrive at

$$H_0(\zeta) \sim -\frac{C_1}{4}\frac{\ln\zeta}{\zeta} \sim -\frac{C_1}{2}\frac{\varepsilon\,\ln\varepsilon}{\widetilde{r}^2} + O\left(\varepsilon\,C_1\frac{\ln\widetilde{r}}{\widetilde{r}^2}\right), \tag{40}$$

where only the leading order term is shown since $|\varepsilon \ln \varepsilon| \gg \varepsilon$ for $\varepsilon \ll 1$. Therefore, for $\widetilde{r} \gg \varepsilon^{1/2}$, the asymptotics of (39) reads

$$\widetilde{\psi}(\widetilde{r}, \theta) = -\frac{C_1}{2}\varepsilon \ln \varepsilon \, \widetilde{r}^{1/2} \cos\frac{\theta}{2} + C^{(c)} \widetilde{r}^{5/2} \cos\frac{5\theta}{2}, \tag{41}$$

which determines the value of the constant $C_1 = 2\sqrt{2}/(\varepsilon \ln \varepsilon)$ and thus $C^{(c)} = -\sqrt{2}/(15\varepsilon \ln \varepsilon)$. Clearly, the first term dominates for $\varepsilon^{1/2} \ll \widetilde{r} \ll |\varepsilon \ln \varepsilon|^{1/2}$; note that the minimum of $|\varepsilon \ln \varepsilon|^{1/2}$ is at $\varepsilon = e^{-1}$, so this defines a non-vanishing $O(1)$ interval of applicability of the inviscid solution.

Of course, the above key part (39) of the solution (32) does not satisfy the boundary conditions (17,31b) everywhere, which is due to the development of boundary layers, cf. Figure 4, both near the impact plate—jet-like flow due to the no-slip boundary condition constructed in Appendix A—and near the interface—ejecta-type behavior due to vanishing along-the-interface velocity, which will be discussed in Sec. VI. However, because the boundary layers are thin for early times, Eq. (39) gives a reasonable approximation for the vertical (normal the interface) velocity, which will be used in Sec. VI C. In order to get a solution uniformly valid both in the inviscid region and in the boundary layers near the solid wall $\theta = \pi$ and interface $\theta = 0$ one needs many Θ_p-modes (35). Note that the boundary layer near the interface is determined by the following scaling near the interface:

$$\widetilde{r} = \delta \widehat{r}, \ \theta = \gamma \widehat{\theta}, \ \varepsilon/(\delta^2\gamma^2) = 1, \ \delta \gg \varepsilon^{1/2}, \ \gamma \ll 1; \tag{42}$$

e.g., for $\widehat{r} = O(1)$, the scaling (42) reduces to $\theta = \varepsilon^{1/2}\widehat{\theta}$; in general, the boundary layer scales as $\gamma = \varepsilon^{1/2}/\delta$, i.e., its thickness becomes narrower with distance $\widetilde{r}$.

D. Pressure

The established value $n = 5/2$ in the Stokes limit makes sense since the corresponding pressure $p \sim \widetilde{r}^{1/2}$ is consistent with the inviscid solution (19)—the pressure in the viscous region cannot be more singular than in the inviscid region, cf. the left-hand side of (31a) and also the discussion in Appendix B. Thus, the pressure scaling does not change between the viscous and inviscid regions and should be the same in both regions. The general solution of (30) is of the form $\widetilde{p}(\widetilde{r}, \theta) = \widetilde{r}^{n-2}\,\pi(\theta)$, with $\pi(\theta)$ given by

$$\pi(\theta) = D_1 \cos(2-n)\theta + D_2 \sin(2-n)\theta, \tag{43}$$

where $n = 5/2$, $D_1 = 0$, and D_2 will be determined Sec. VI. Notably, the pressure gradient is singular as in the inviscid case, i.e., forces involved at the edge are infinite, which is due to the use of an incompressible approximation—however, because of the infinitely small masses involved around the singularity, the resulting velocities are finite $\mathbf{v} \sim r^{3/2}$ and thus overall the physics makes sense to the extent it can in the incompressible approximation.

E. Further observations

Finally, while here we constructed the solution assuming that the liquid wets the plate perfectly, i.e., the contact angle is $\theta = 0$ as assumed in Sec. II, we would like to point out the existence of non-singular solutions of the Stokes equation in the regions of angle span different from π. This fact is also known from the study of Moffatt[53] and here would physically imply that the contact angle between the liquid and the solid is different from zero so that the boundary conditions (31) would be prescribed at some $\theta \neq 0$ as opposed to $\theta = 0$ required by the Kutta-Joukowsky condition used in previous studies.[32,35–37] Physically, this is possible since in the Stokes region a fluid is inertialess as opposed to the reasoning behind the justification for applying the Kutta-Joukowsky condition implicitly based on fluid inertia.

From the constructed solution, it follows that the velocity field is time-independent in the Stokes region after we revert to the unscaled (physical) variables:

$$\mathbf{v} \sim r^{3/2}. \tag{44}$$

Given the power exponent 3/2 of the velocity field, we are now in a position to address the question as to when the nonlinear inertia terms become important. As follows from equation (24), by comparing the linear and nonlinear inertia terms, the corresponding critical time scales as $\tau_c \sim \widetilde{r}^{-2}$, which means that for small times near the edge, $\widetilde{r} \ll 1$, this critical time is large and thus our short time analysis is justifiably governed by linear equations (27). In summary, we determined the existence of a uniformly valid self-similar solution (34) spanning from the Stokes to the inviscid flow regions—this, however, is not a surprise as, based on the dimensional analysis, in the neighborhood of the edge there is no independent length scale as $l_\nu/l \ll 1$, where $l_\nu = \sqrt{\nu\, t}$ is the viscous length scale.

VI. EJECTA

A. Inviscid solution

Given the above understanding of the velocity and pressure fields, we are now in a position to deduce the dynamics of ejecta at early times in the inviscid region. This outer (inviscid) solution corresponds to $\varepsilon = 0$ in (31) thus yielding

$$\underline{-\widetilde{p}} = \frac{\tau^{1/4}}{We}\,[2\,h_{\widetilde{r}} + \widetilde{r}\,h_{\widetilde{r}\widetilde{r}}]\,, \tag{45a}$$

$$\underline{h_\tau - \frac{1}{2}\frac{\widetilde{r}}{\tau}\,h_{\widetilde{r}}} = -\tau^{-3/4}\frac{1}{\widetilde{r}}\left[\underline{\frac{\partial\widetilde{\psi}}{\partial\widetilde{r}}} + \frac{\partial\widetilde{\psi}}{\partial\theta}\,h_{\widetilde{r}}\right], \tag{45b}$$

where only the underlined terms survive at the leading order. Since the velocity of the interface must be equal to that of the fluid, we require $h(\tau,\widetilde{r}) = \tau^{1/4}\widehat{h}(\widetilde{r})$, so that the underlined terms in (45b) are balanced:

$$\widetilde{p} = 0, \tag{46a}$$

$$\frac{1}{4}\widehat{h} - \frac{1}{2}\widetilde{r}\,\widehat{h}_{\widetilde{r}} = -\frac{1}{\widetilde{r}}\frac{\partial\widetilde{\psi}}{\partial\widetilde{r}}, \tag{46b}$$

which implies that at the leading order the pressure vanishes, $\widetilde{p} = 0$, which makes sense as the interfacial departures are small and therefore capillary pressure contributes negligibly; also the leading order h is determined by Eq. (46b). Given the solution for the inviscid velocity field (14), the free interface solution scales as $\widehat{h} \sim \widetilde{r}^{-3/2}$, which in the physical space reads

$$h \sim t\,r^{-3/2}, \tag{47}$$

i.e., it tends to zero as $t \to 0$, as it should be, but develops a singularity for $r \to 0$ and $t > 0$ consistent with the previous finding.[54]

There are three key observations to make. First, we showed the self-similar nature of h in the inviscid region provided

$$\widetilde{r} \gg \tau^{1/2}\,We^{-2}, \tag{48}$$

i.e., under this condition we can neglect the capillary pressure terms in (45a), which follows from (45a) after linearization of the pressure term, $\widetilde{p}|_{\theta=h(t,r)} = \widetilde{p}|_{\theta=0} + \widetilde{p}_\theta|_{\theta=0}\cdot h(t,r) + \ldots$. Second, it is clear that one cannot match the interface in the self-similar inviscid approximation to the Kutta-Joukowsky condition as $h \to \infty$ for $r \to 0$ for $t > 0$ based on the result (47). Third, one needs to reconcile previous uses of Yakimov's scaling[19,32,34–36] and the implications of the present work. Despite the difference between Yakimov's scaling (20) and the one deduced here (23), it is remarkable that the scaling for the free surface profile (47) is consistent with what Yakimov's scaling (20) would predict at the free surface even though (47) was arrived at without Yakimov's scaling. Namely, (47) gives $y \sim t\,x^{-1/2}$ for the interface shape and since both spatial coordinates are equivalent near the edge $x \sim y$, then $x, y \sim t^{2/3}$ as per (20). However, this does not mean that Yakimov's scaling is appropriate for scaling the NSEs as shown in Sec. IV, in particular because in the limit $t \to 0$ it does not allow one to recover the inviscid solution (4) constructed by complex variable analysis. In fact, while Yakimov[19] came up with his scaling based on the dimensional analysis,[55] it was shown

later[32,34] that the choice of Yakimov's scaling can also be seen as dictated by the nonlinearity of the interfacial boundary condition and the condition (5) near the edge, i.e., based on a different argument. Therefore, according to the physics of the problem at early times discussed in the Introduction, when nonlinearity is not important the scaling does not have to comply with the restriction imposed by nonlinearity (though the condition (5) is still respected) thus allowing one to properly account for the viscous effects and the limit $t \to 0$ as done in the present study with the help of the scaling (23).

In this context, it is worth mentioning how Yakimov's scaling was tested in the literature. The self-similar solution from the work of Iafrati and Korobkin,[32] derived based on Yakimov's scaling and constructed numerically, was later compared[35,36] to fully-nonlinear potential flow numerical simulations and tested based on the predictions for the free surface shape as well as for the pressure distribution on the plate. Also, Iafrati and Korobkin[36] compared short time history of the impacting disk velocity to the experiments by Glasheen and McMahon.[56] And, finally, Peters *et al.*[34] compared numerical solution of the full (non-scaled) potential problem to the analytical solution at $t = 0$, though both solutions were constructed without recourse to Yakimov's scaling (20). In none of the above works, the Yakimov self-similarity of the velocity field was verified in the bulk, which can be understood based on the fact that the leading order solution for the velocity field is time-independent for short times right after the impact. Indeed, the new scaling (23) for $|\boldsymbol{r}| \gg \varepsilon^{1/2}\tau^{1/2}$, i.e., outside the viscous boundary layer, gives (5), which is consistent with what Yakimov's scaling (20) predicts in the far field[32] and thus both scalings (20) and (23) give the leading order term independent of time $\mathbf{v}(t, x, y) \to \mathbf{v}_0(x, y)$ as $t \to 0$, where $\mathbf{v}_0(x, y)$ is given by (15). Despite that the leading order term $\mathbf{v}_0(x, y)$ is time-independent, the leading order non-zero term of the interface elevation (47) is time-dependent. In addition, one must point out that in all the above mentioned works the singularity at $t \to 0$ was not resolved since all the constructed numerical solutions apply for times $t > t_0 > 0$ with some finite t_0. In contrast, the analytical solution constructed in the present work, valid for early times when the plate displacement can be neglected as it was done in the work of Iafrati and Korobkin,[32] resolves both singularities near the edge $r \to 0$ and as $t \to 0$. In summary, despite the difference in the scalings (20) and (23), the new scaling (23) is consistent with what Yakimov's scaling predicts in the far field and at the interface in the inviscid region as explained above.

B. Stokes solution

Next let us consider the Stokes approximation. To demonstrate the self-similar nature of h, note that the leading order terms in (31) are as shown underlined

$$\underline{-\widetilde{p} + \frac{\varepsilon}{\widetilde{r}}\left(\frac{1}{\widetilde{r}}\widetilde{\psi}_\theta - \widetilde{\psi}_{\widetilde{r}\theta}\right)} = \frac{\tau^{1/4}}{We}\left[2\,h_{\widetilde{r}} + \widetilde{r}\,h_{\widetilde{r}\widetilde{r}}\right], \tag{49a}$$

$$\frac{\varepsilon}{\tau^{3/4}}\underline{\left(\frac{1}{\widetilde{r}^2}\widetilde{\psi}_{\theta\theta} + \frac{1}{\widetilde{r}}\widetilde{\psi}_{\widetilde{r}} - \widetilde{\psi}_{\widetilde{r}\widetilde{r}}\right)} = 0, \tag{49b}$$

$$\underline{h_\tau - \frac{1}{2}\frac{\widetilde{r}}{\tau}h_{\widetilde{r}}} = \underline{-\frac{\tau^{-3/4}}{\widetilde{r}}\left[\widetilde{\psi}_\theta\,h_{\widetilde{r}} + \widetilde{\psi}_{\widetilde{r}}\right]}. \tag{49c}$$

The normal dynamic condition (49a) indicates that the right-hand-side term $O(\tau^{1/4})$ is negligible since we consider the solution to leading order in time having self-similar structure, while the pressure and the viscous normal stresses on the left-hand-side of (49a) balance each other—note that the pressure $\widetilde{p} \sim \widetilde{r}^{1/2}$ and $\widetilde{\psi} \sim \widetilde{r}^{5/2}$ in the viscous case—and thus determine the constant $D_2 = -\sqrt{2}/\ln\varepsilon$ in (43) via the linearization of $\widetilde{p}$ and $\widetilde{\psi}$ around $\theta = 0$:

$$-\widetilde{p}_\theta|_{\theta=0}\cdot h + \frac{\varepsilon}{\widetilde{r}}\left(\frac{1}{\widetilde{r}}\widetilde{\psi}_{\theta\theta} - \widetilde{\psi}_{\widetilde{r}\theta\theta}\right)\Big|_{\theta=0}\cdot h = 0, \tag{50}$$

where we took into account that $\widetilde{p}|_{\theta=0} = 0$ and $\Theta'(0) = 0$ based on the knowledge of the solution (38) with $C^{(s)} = 0$. The determined leading order pressure, $\widetilde{p} = \sqrt{2}\ln^{-1}\varepsilon\,\widetilde{r}^{1/2}\sin(\theta/2)$ together

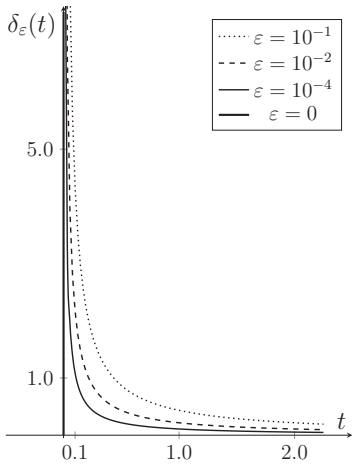

FIG. 5. Delta-sequence $\delta_\varepsilon(t) = -t^{-1}/\ln\varepsilon$. Dirac delta-function $\delta_D(t)$ corresponds to $\varepsilon = 0$.

with the scaling (23) gives the following formula for the pressure in the physical space

$$p = \rho\, V_0 \sqrt{2\,l}\, \frac{t^{-1}}{\ln\varepsilon}\, r^{1/2} \sin\frac{\theta}{2}, \tag{51}$$

i.e., it is singular at $t = 0$, which is a consequence of the incompressible flow approximation. This formula is nothing more, but the pressure from the classical potential flow solution (19) with the only difference in that the Dirac delta function $\delta_D(t)$ is now replaced by the delta-sequence[57] $\delta_\varepsilon(t) = -t^{-1}/\ln\varepsilon$, cf. Figure 5. Since the formula for pressure (51) applies to both viscous and inviscid regions, then the pressure distribution in space is the same as from the potential flow solution,[58] but its sudden time-dependence $\delta_D(t)$ is smoothened by the viscosity producing $\delta_\varepsilon(t)$ such that in the limit of zero viscosity it converges to the Dirac delta-function:

$$\lim_{\varepsilon\to 0} \delta_\varepsilon(t) = \delta_D(t). \tag{52}$$

Hence, one must recover the inviscid potential solution (4) and the corresponding governing equation (1) when taking the limit $t \to 0$ in the Navier-Stokes equations in the weak topology sense, i.e., almost everywhere except for the infinitely thin boundary layer, in the same way as the Euler equations are recovered from the NSEs in the limit of zero viscosity.[59] Indeed, based on the definition of the delta-sequence (and Delta-function) as a distribution[57]

$$(\delta_D(t), \phi(t)) = \phi(0) \tag{53}$$

for any test function $\phi \in C_0^\infty$ (i.e., infinitely differentiable and with compact support) one finds

$$(\delta_\varepsilon, \phi) = -\frac{1}{\ln\varepsilon}\int_{-\tau_1(\varepsilon)}^{\tau_2(\varepsilon)} \frac{\phi(t)}{t}\mathrm{d}t = -\frac{1}{\ln\varepsilon}\int_{-\tau_1(\varepsilon)}^{\tau_2(\varepsilon)} \frac{\phi(t)-\phi(0)}{t}\mathrm{d}t - \frac{1}{\ln\varepsilon}\int_{-\tau_1(\varepsilon)}^{\tau_2(\varepsilon)} \frac{\phi(0)}{t}\mathrm{d}t, \tag{54}$$

where in the limit $\tau_{1,2}(\varepsilon) \to 0$ as $\varepsilon \to 0$ the first integral vanishes since $\phi(t) - \phi(0) = O(t)$ and the second integral gives

$$-\frac{\phi(0)}{\ln\varepsilon}\ln\frac{\tau_2(\varepsilon)}{\tau_1(\varepsilon)} = \frac{\phi(0)}{\ln\varepsilon}\ln\frac{\tau_1(\varepsilon)}{\tau_2(\varepsilon)}, \tag{55}$$

that is by appropriately choosing the interval of integration, $\tau_1(\varepsilon)/\tau_2(\varepsilon) = \varepsilon$ as $\varepsilon \to 0$, one proves that our delta-sequence $\delta_\varepsilon(t)$ converges to the Dirac delta-function $\delta_D(t)$, since $\lim_{\varepsilon\to 0}(\delta_\varepsilon, \phi) = \phi(0)$. Note that the asymmetry of the time interval $(-\tau_1(\varepsilon), \tau_2(\varepsilon))$ is consistent with the physical asymmetry of the impact event in time. Finally, as follows from (51), the lower the viscosity, the more singular the pressure, i.e., viscosity plays a "smoothening" role, which is natural as it introduces higher-order derivative terms in (27). As is the case for any other self-similar solutions, e.g., the Jeffrey-Hamel flow in a converging channel,[41] the one constructed above is an idealization in the sense that real

fluid properties (such as compressibility and finite non-zero surface tension) cannot support the existence of the singularity and thus is valid for $t > 0$ only. However, as generally known,[60] self-similar solutions are useful constructions which capture the flow structure "in large" and thus provide reasonable approximations to observable flows away from singularities.

Since the normal and tangential interfacial conditions drop out from our consideration of the ejecta evolution, its shape $h(\widetilde{r})$ is determined from the kinematic boundary condition balancing the interface and fluid velocities:

$$h_\tau - \frac{1}{2}\frac{\widetilde{r}}{\tau}\,h_{\widetilde{r}} = -\frac{\tau^{-3/4}}{\widetilde{r}}\left[\widetilde{\psi}_{\widetilde{r}} + h\,h_{\widetilde{r}}\,\widetilde{\psi}_{\theta\theta}\right], \tag{56}$$

where we also linearized $\widetilde{\psi}$ around $\theta = 0$. If one neglects the nonlinear term $h\,h_{\widetilde{r}}\,\widetilde{\psi}_{\theta\theta}$ in the above equation, which is of higher order in time $O(\tau^{1/2})$ as can be seen *a posteriori*, then from the knowledge of $\widetilde{\psi} = c\,\widetilde{r}^{5/2}$, $c = -4\,C^{(c)}$, at $\theta = 0$ it follows that $h = a(\tau)\widetilde{r}^{1/2}$ with $a(\tau)$ found from the linear equation

$$\frac{\mathrm{d}a}{\mathrm{d}\tau} - \frac{a}{4\tau} = -\frac{5\,c}{2\,\tau^{3/4}}, \tag{57}$$

yielding $a(\tau) = -\frac{5}{2}\,c\,\tau^{1/4}\,\ln\tau$. The latter implies that

$$h = -\frac{2\sqrt{2}}{3\,\varepsilon\,\ln\varepsilon}\,\widetilde{r}^{1/2}\,\tau^{1/4}\,\ln\tau, \tag{58}$$

i.e., $h \to 0$ as $\tau \to 0$ in the self-similar variables $(\tau, \widetilde{r})$, but in the physical space $h \sim r^{1/2}\ln t$, which makes sense for non-zero times, i.e., the limits $t \to 0$ and $r \to 0$ are distinguished here. Of course, as $\ln\tau$ becomes significant for short times, the nonlinear term in (56) "kicks in" and regularizes the solution. *A posteriori* the above result proves the assumption made before (cf. Sec. II) that $\widetilde{r}\,h_{\widetilde{r}} \ll 1$ for small $\widetilde{r}$. However, the interface curvature does not vanish as $\widetilde{r} \to 0$, cf. (10)—the limits $\widetilde{r} \to 0$ and $\tau \to 0$ are distinguished. This implies that for any $\tau > 0$, no matter how small, the nontrivial pressure and normal viscous stresses for $\widetilde{r} > 0$ curve the interface and are balanced by the capillary pressure in the non-self-similar subregion.

C. General solution and further observations

Given the knowledge of the time-dependence of h in self-similar variables, we can comment on the validity of the self-similar solution in the presence of surface tension based on equation (49a). Namely, the capillary pressure term on the right-hand side of (49a) is negligible over the same distances as defined by (48) obtained in the inviscid approximation—one can arrive at this condition by performing the same type of analysis as for (48). Since we are working with small times and in the case of large Weber numbers, this sets the region of validity of the self-similar solution. For smaller $\widetilde{r}$'s the solution is *not* self-similar in all variables, $\widetilde{\psi}$, $\widetilde{p}$, and h, and should encompass both viscous and surface tension effects.

Construction of the solution for the interfacial slope $h(\tau, \widetilde{r})$ at early times, which is valid both in the viscous and inviscid regions amounts to solving Eq. (56) for $h(t, r)$ with the determined velocity field (39) and with the boundary condition $h(\tau, 0) = 0$ in view of the assumed zero angle at which the ejecta meets the plate (Sec. II) and the initial condition $h(0, \widetilde{r}) = 0$. This results in a uniformly valid solution matching the Stokes (58) and inviscid (47) scalings shown in Figure 6, where the locations of the highest ejecta elevation $y = r\sin h \simeq r\,h$ and velocity $\left(x_t^2 + y_t^2\right)^{1/2} = r\,h_t$ in the Cartesian frame of reference are indicated by filled circles and correspond to the points where $h + r\,h_r = 0$. In summary, in self-similar variables, different parts of h evolve on different time scales:

$$\text{inviscid}: \;\; h \sim \tau^{1/4}\widetilde{r}^{-3/2}, \;\; \widetilde{r} \gg \varepsilon^{1/2} \tag{59a}$$

$$\text{Stokes}: \;\; h \sim \tau^{1/4}\ln\tau\,\widetilde{r}^{1/2}, \;\; \widetilde{r} \ll \varepsilon^{1/2}, \tag{59b}$$

i.e., the time growth of h is different in the inviscid and viscous regions.

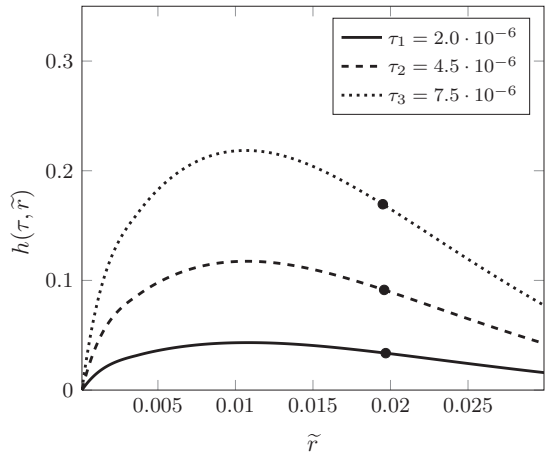

FIG. 6. Ejecta evolution $\theta = h(\tau, \widetilde{r})$ in the self-similar variables $(\tau, \widetilde{r})$ for $\varepsilon = 10^{-4}$. Filled circles denote the locations of the highest ejecta elevation and velocity in the Cartesian coordinates.

To illustrate that the above general theory works at early times, let us consider a concrete example. Suppose $l = 10^{-2}$ m, $V_0 = 1$ m/s, $\nu = 10^{-6}$m^2/s, and $\sigma = 7.2 \times 10^{-2}$ N/m which gives $Re_0 = 10^4$ ($\varepsilon = 2 \times 10^{-4}$) and $We = 1.4 \times 10^2$. According to the presented analysis, we get the peak of the ejecta to be $h = O(10^{-1})$ and located at $\widetilde{r} = O(10^{-2})$, which at the time $t = 10^{-7}$ s (translating into $\tau = O(10^{-5})$) corresponds to $\overline{r} = O(10^{-3})$ mm and the physical ejecta height $\overline{r} \sin h = O(10^{-4})$ mm, i.e., the ejecta deflection from the horizontal is not yet substantial on this time scale as opposed to the prediction from the classical potential flow solution. Also, one can distinguish three regions

$$\text{inviscid}: \ \overline{r} \gg \sqrt{V_0 l t \varepsilon}, \tag{60a}$$

$$\text{viscous}: \ \overline{r} \sim \sqrt{V_0 l t \varepsilon}, \tag{60b}$$

$$\text{Stokes}: \ \overline{r} \ll \sqrt{V_0 l t \varepsilon}, \tag{60c}$$

where the viscous length scale is $\overline{r} \sim \sqrt{V_0 l t \varepsilon} \simeq 10^{-1}$ mm for $t = 1$ ms.[61] Finally, in order to neglect surface tension, as done in the analysis of Sec. VI, over the times $t \leq 1$ ms, cf. Eq. (48), we need

$$\overline{r} \gg t \frac{\sigma^2}{\rho^2 V_0^3 l^2} = 10^{-8} \text{ mm}, \tag{61}$$

which is clearly satisfied even in the Stokes region.

VII. CONCLUSIONS

In this work, we presented the analysis of the early time evolution of ejecta in the water impact problem, which turns to be a singular perturbation problem described by linear equations. The self-similar solution for the velocity field is expressed analytically in terms of the confluent hypergeometric functions. It transpires that the viscosity effects contribute to the solution at leading order due to the singular perturbation nature of the problem. In the course of construction of the solution, first the standard assumptions for the existence of the inviscid approximation are revisited, which clarifies the previously known interpretation of the self-similarity of this inviscid solution near the plate edge. Second, the new scaling (23) of the structure of the solution near the plate edge is determined, with the help of which the viscous solution near the edge is constructed analytically and proves to be self-similar and uniformly valid in between the Stokes, $\mathbf{v} \sim r^{3/2}$, and inviscid, $\mathbf{v} \sim r^{1/2}$, regions. This new self-similar solution allows us to determine the early

time-evolution of the ejecta with the asymptotics in the Stokes, $h(r,\, t) \sim r^{1/2} \ln t$, and inviscid, $h(t,\, r) \sim t\, r^{-3/2}$, regions and also to reveal the *ad hoc* nature of the Kutta-Joukowsky condition used in previous studies. Altogether, the constructed here analytical solution resolves both "$t \to 0$" and "$r \to 0$" singularities in the classical pressure-impulse theory. At the philosophical level, the present study validates, in the viscous approximation, the assumption built into the Wagner's model[6] that the dependence of the flow on time follows a law of similarity with the free boundary of the fluid continuously expanding away from the solid surface.

Open questions requiring further study include construction of a uniformly valid non-self-similar solution on the scales $\widetilde{r} \lesssim \tau^{1/2}\, We^{-2}$, and resolution of the infinite pressure gradients by performing the analysis in the compressible liquid case. To extend the analysis to later times, it might help to construct next order (in time) asymptotic approximations and thus to account for a nonlinear evolution of the ejecta.

One must note that ejecta naturally occurs not only in the solid-liquid impacts, but also in the liquid-liquid impact such as the drop splash problem.[15,62,63] Predicting the ejecta properties at early times in the latter problem is instrumental for analyzing the instability responsible for the crown formation.[63,64] In the inviscid analysis,[64] using mass, momenta, and energy conservation in the control volume approximation (i.e., neglecting the details of the flow, but taking into account all these conservation laws in the integral sense) along with some geometric constraints, it was shown that the evolution of ejecta at early times obeys $\theta_e \sim t^{1/2}$, $v_e \sim \theta_e$, and $h_e \sim \theta_e^2$ for the ejecta angle, velocity, and thickness, respectively, which is consistent with the fact that any materialistic ejecta cannot have infinite speed as $t \to 0$ and, on the contrary, should start from rest. Because in this case the heavier fluid is accelerating into the lighter one, the linear stability analysis of liquid sheet edges[65,66] shows that an instability must first appear at the acceleration stage via the Richmyer-Meshkov mechanism. Understanding how ejecta evolution is affected by viscosity is crucial for accurate prediction of the crown structure in the drop splash problem in the same vein as the present study showed the importance of viscosity in the water impact problem.

ACKNOWLEDGMENTS

The author gratefully acknowledges stimulating discussions on the subject with Professor Vladislav Vasil'evich Pukhnachev during his visit at UCSB in 2010. This work was partially supported by the National Science Foundation (NSF) CAREER award under Grant No. 1054267, American Chemical Society (ACS) Petroleum Research Fund under Grant No. 51307-ND5, and the Natural Sciences and Engineering Research Council of Canada (NSERC) under Grant No. 6186.

APPENDIX A: STRUCTURE OF THE WALL JET

The inviscid solution discussed in the Introduction and Sec. III defines the "outer" solution. The idea is to find its "viscous" substructure close to the plate—the viscous jet under the plate, which should "extend" the viscous effects to the ejecta. Thus, as a first step towards understanding the origin of ejecta, recall that upon the impact a wall jet[67] is driven by the pressure gradient between the high pressure region beneath the plate center and the low pressure region outside the plate $\Pi = -\rho\, \phi|_{t=+0}$, $\phi = \mathrm{Re} f(z)$: thus the jet propagates from the plate center toward the edges. As follows from (14), the x-velocity distribution near the plate, i.e., for $y \ll x$ and away from edges, is given by

$$u = V_0 \frac{x}{\sqrt{l^2 - x^2}} + O(y^2), \tag{A1}$$

where the leading order part will be denoted by $U(x)$.

In the Cartesian (x, y')-coordinates in the frame of reference moving with the plate, $y' = y + V_0\, t$, the boundary layer approximation for small times right after the impact reads

$$\frac{\partial u}{\partial t} + V_0 \frac{\partial u}{\partial y} = -\frac{1}{\rho}\, p_x + \nu \frac{\partial^2 u}{\partial y'^2}, \tag{A2a}$$

$$\int_{-0}^{+0} p\,\mathrm{d}t = \rho V_0 \sqrt{l^2 - x^2} = \Pi, \tag{A2b}$$

where the presence of the additional convective term $V_0\,\partial u/\partial y$ is due to the fact that in the moving frame of reference observation of the time-rate of change of u depends on V_0, since u is a function of y. The condition (A2b) states that the boundary layer is driven impulsively by the pressure distribution near the lower surface of the plate, $\Pi = -\rho\,\phi|_{t=+0}$. Also, we neglected the nonlinear inertia terms following the argument in Sec. IV,[68] so that the equation is essentially of the heat (parabolic) type with an impulsive driving term, $-p_x/\rho$. The appropriate boundary conditions are the no-slip at the wall, $y' = 0$: $u = 0$, and the matching condition to the inviscid solution, $y' \to -\infty$: $u \to U(x)$ given by (A1). The boundary layer approximation formally fails near the edge, cf. region 3 in Figure 4, and similar to the flow around the leading edge of a flat plate[46,47] is not matchable to the Stokes solution.

Equation (A2) is amenable to analysis with the Laplace transform in the time variable, $\mathcal{L}(u) = \widehat{u}(\lambda) = \int_0^{+\infty} u(t)\,e^{-\lambda t}\,\mathrm{d}t$, producing

$$u(t, x, y') = U(x)\left[1 + \frac{y'}{2\sqrt{\nu\,t}}\,e^{y'\frac{V_0^2}{2\nu}}\int_0^t e^{-\frac{V_0^2}{4\nu}t} e^{-\frac{y'^2}{4\nu t}}\,t^{-3/2}\,\mathrm{d}t\right], \tag{A3}$$

where we used the formula $\rho^{-1}\,\mathrm{d}\Pi/\mathrm{d}x = -U(x)$ for the pressure gradient from the inviscid approximation. Expression (A3) tells us that for any fixed $y' > 0$, no matter how small it is, as $t \to +0$ we have $u \to U(x)$, and as $t \to +\infty$, $u \to 0$, which illustrates the $O(1)$ time-dependence, e.g., in the laboratory frame of reference $V_0 = 0$:

$$u(t, x, y') \sim \begin{cases} U(x)\left[1 + \frac{2}{y'}\sqrt{\frac{\nu t}{\pi}}e^{-\frac{y'^2}{4\nu t}}\right], & \frac{(-y')}{2\sqrt{\nu\,t}} \gg 1, \\ U(x)\frac{(-y')}{\sqrt{\pi\,\nu\,t}}, & \frac{(-y')}{2\sqrt{\nu\,t}} \ll 1. \end{cases} \tag{A4}$$

Note that, as opposed to the standard wall jet,[69,70] this jet is driven by the pressure gradient between the high pressure region beneath the plate center and the low pressure region outside the plate. As follows from (A3), its thickness grows as the viscous length scale $l_\nu = \sqrt{\nu\,t}$, which is analogous to the first Stokes problem,[71] and thus the vorticity generated due to the no-slip boundary condition at the plate diffuses at the distance on the order of l_ν—this is the key fact learned from the above analysis, which is used in Sec. IV. As follows from the discussion in Sec. V, the inviscid solution is time-independent at leading order in time, and thus the leading order time-dependence of the overall solution for short times comes from the boundary layer, cf. (A4). That is, the inviscid solution is set everywhere at $t = +0$ and for $t > 0$ it is modified by the diffusion of the boundary layer (wall jet) into it.

APPENDIX B: GENERAL SOLUTION OF (27)

The solution to (27) can be constructed using separation of variables, $\widetilde{\psi}(\widetilde{r}, \theta) = R(\widetilde{r})\,\Theta(\theta)$, where the function $\Theta(\theta)$ should satisfy the no-slip boundary conditions at the plate

$$\theta = -\pi : \ \Theta = \Theta' = 0, \tag{B1}$$

and the tangential dynamic component (31b) of the free surface boundary conditions:

$$\theta = 0 : \ -\widetilde{\psi}_{\widetilde{r}\widetilde{r}} + \frac{1}{\widetilde{r}}\widetilde{\psi}_{\widetilde{r}} + \frac{1}{\widetilde{r}^2}\widetilde{\psi}_{\theta\theta} = 0. \tag{B2}$$

Given the form of the solution $\widetilde{\psi}(\widetilde{r}, \theta) = R(\widetilde{r})\,\Theta(\theta)$, the dynamic tangential boundary condition tells us that at $\theta = 0$ for $R(\widetilde{r}) = \widetilde{r}^n$ either (a) $n = 0, 2$ with $\Theta'' = 0$ and Θ being arbitrary or (b) $n \neq 0, 2$ with the condition

$$\theta = 0 : \ (2 - n)\,n\,\Theta + \Theta'' = 0; \tag{B3}$$

if, however, $R(\widetilde{r})$ is a general non-polynomial function, then $\Theta = \Theta'' = 0$ at $\theta = 0$.

Problem (27) is clearly of singular perturbation type as the small parameter ε multiplies the higher order derivative term. Singular behavior is also obvious from the form of the boundary conditions (31) and the change in the boundary conditions on the plate (17) from viscous to inviscid one in the limit $\varepsilon \to 0$. Thus, one can think of the structure of the solution to (27) in terms of inner and outer solutions. The inner solution corresponds to $\widetilde{r} = O(\varepsilon^{1/2})$. However, in view of the linearity of the problem (27), we can construct its exact general solution valid for all $\widetilde{r}$ and thus we will deal with the problem in the original (unscaled) variables (27). Separation of variables $f(\widetilde{r}, \theta) = R_f(\widetilde{r})\,\Theta_f(\theta)$ produces

$$\Theta_f'' + \beta^2\,\Theta_f = 0,\ \widetilde{r}^2 R_f'' + \widetilde{r}\left(1 + \frac{\widetilde{r}^2}{\varepsilon}\right) R_f' + \left(\frac{3}{2}\frac{\widetilde{r}^2}{\varepsilon} - \beta^2\right) R_f = 0. \tag{B4}$$

While the relevant solution of the first of these equations is $\Theta_f(\theta) = Ae^{i\beta\,\theta} + Be^{-i\beta\,\theta}$ with $\beta > 0$, the second one can be analyzed via the change of variables $R_f(\widetilde{r}) = \xi^k\,\eta(\xi)$ with $\xi = \widetilde{r}^2$ and $k = \pm\beta/2$; with further rescaling $\xi = -2\,\varepsilon\,\zeta$, we arrive at the Kummer's equation:[51,72]

$$\zeta\,\eta'' + (\widehat{b} - \zeta)\,\eta' - \widehat{a}\,\eta = 0,\ \text{where}\ \widehat{b} = 1 + 2k,\ \widehat{a} = \frac{1}{2}\left(\frac{3}{2} + 2k\right), \tag{B5}$$

the solution of which is given in terms of confluent hypergeometric functions[73] of the first $M(\widehat{a}, \widehat{b}, \zeta)$ and second $U(\widehat{a}, \widehat{b}, \zeta)$ kinds, $\eta_k(\zeta) = C_{1k}\,M_k(\widehat{a}, \widehat{b}, \zeta) + C_{2k}\,U_k(\widehat{a}, \widehat{b}, \zeta)$, corresponding to two different $k_{1,\,2} = \pm\beta/2$.

Now, let us make a few preliminary observations, which will facilitate further construction of the solution. First, observe that due to the fractional exponent $n = 1/2$ in the inviscid solution (14), the corresponding solution in the Stokes region satisfying (B1) and (B3), should be also determined with fractional n:[74]

$$n - \frac{1}{2} \in \mathbb{Z}:\ \Theta(\theta) = C_1\,[n\,\cos(2-n)\theta - (n-2)\,\cos n\theta] + C_2\,[\sin n\theta + \sin(2-n)\theta], \tag{B6}$$

so that both inviscid and Stokes solutions can be matched through the general viscous solution. The lowest possible values of $n \geq 1$, i.e., leading to a non-singular velocity field, are 3/2 and 5/2. The value 3/2 would lead to a singular $h(t, r)$ as one can observe from (31c) and thus should be excluded. Therefore, the lowest possible value is 5/2 which makes sense as it balances $\widetilde{p} \sim \widetilde{r}^{1/2}$ and $\widetilde{\psi} \sim \widetilde{r}^{5/2}$ in the normal dynamic boundary condition (31a). In summary, in terms of the function f the leading order solution for $\widetilde{r} \to \infty$ is $f \sim \widetilde{r}^{-3/2}$, which implies that $\widetilde{\psi} \sim \widetilde{r}^{1/2}$ as it should be in the inviscid region (14) and, as $\widetilde{r} \to 0$, $f \sim \widetilde{r}^{1/2}$, so that $\widetilde{\psi} \sim \widetilde{r}^{5/2}$ in the Stokes flow region.

In order to select the proper solution to (27), note that based on the knowledge of the inviscid (14) solution, the dominant asymptotics should be $R_f \sim \widetilde{r}^{-3/2}$. From the analysis of the asymptotics of the general solutions $\eta_k(\zeta)$ for $\widetilde{r} \ll \varepsilon^{1/2}$ (Stokes) and $\widetilde{r} \gg \varepsilon^{1/2}$ (inviscid), we find that the confluent hypergeometric function of the first kind $M(\widehat{a}, \widehat{b}, \zeta)$ has the following asymptotic behavior:

$$\widetilde{r} \ll \varepsilon^{1/2}:\ M(\widehat{a}, \widehat{b}, \zeta) \simeq 1 + \frac{\widehat{a}}{\widehat{b}}\zeta\ \Rightarrow\ R_f \sim \widetilde{r}^{2k}, \tag{B7a}$$

$$\widetilde{r} \gg \varepsilon^{1/2}:\ M(\widehat{a}, \widehat{b}, \zeta) \simeq \frac{\Gamma(\widehat{b})}{\Gamma(\widehat{b} - \widehat{a})}(-\zeta)^{-\widehat{a}} \sim \widetilde{r}^{-\frac{3}{2} - 2k}\ \Rightarrow\ R_f \sim \widetilde{r}^{-3/2}, \tag{B7b}$$

while asymptotics of the confluent hypergeometric function of the second kind can be determined from its general form

$$U(\widehat{a}, \widehat{b}, \zeta) = \frac{\pi}{\sin\pi\,\widehat{b}}\left\{\frac{M(\widehat{a}, \widehat{b}, \zeta)}{\Gamma(1 + \widehat{a} - \widehat{b})\Gamma(\widehat{b})} - \zeta^{1-\widehat{b}}\frac{M(1 + \widehat{a} - \widehat{b}, 2 - \widehat{b}, \zeta)}{\Gamma(\widehat{a})\Gamma(2 - \widehat{b})}\right\}, \tag{B8}$$

thus yielding

$$\widetilde{r} \ll \varepsilon^{1/2}:\ U(\widehat{a}, \widehat{b}, \zeta) \sim \mathrm{sing}\big(\widetilde{r}^{-2k}, 1\big)\ \Rightarrow\ R_f \sim \mathrm{sing}\big(1, \widetilde{r}^{2k}\big), \tag{B9a}$$

$$\widetilde{r} \gg \varepsilon^{1/2}:\ U(\widehat{a}, \widehat{b}, \zeta) \sim (-\zeta)^{-\widehat{a}} \sim \widetilde{r}^{-\left(\frac{3}{2} + 2k\right)}\ \Rightarrow\ R_f \sim \widetilde{r}^{-3/2}, \tag{B9b}$$

where sing-function chooses the most singular of its two arguments. Recall that $k = \pm\beta/2$. Since the lowest value of β is $\beta_0 = 1/2$ and, as will be shown later, $\beta_m = \beta_0 + m$, $m \in \mathbb{N}$ we can exclude negative values of $\beta = -\beta_m$ due to the required asymptotics of $R_f \sim \widetilde{r}^{1/2}$ at $\widetilde{r} \ll \varepsilon^{1/2}$. Also, the confluent hypergeometric function of the second kind $U(\widehat{a}, \widehat{b}, \zeta)$ is not relevant as its asymptotics for $\widetilde{r} \ll \varepsilon^{1/2}$ gives the leading order term $R_f \sim \widetilde{r}^0$ as opposed to the necessary $R_f \sim \widetilde{r}^{1/2}$.

Thus, the general solution for f valid both in the viscous and inviscid regions involves only $M_k(\widehat{a}, \widehat{b}, \zeta) \equiv M(\widehat{a}, \widehat{b}, \zeta)$ corresponding to $k = \beta/2$ and reads

$$R_f(\widetilde{r}) = \widetilde{r}^{2k}\, M\left(-\widetilde{r}^2/(2\varepsilon)\right), \text{ so that } f(\widetilde{r}, \theta) = C_1\, \Theta_f(\theta)\, \widetilde{r}^{2k}\, M\left(-\widetilde{r}^2/(2\varepsilon)\right), \tag{B10}$$

and the stream-function $\widetilde{\psi}(\widetilde{r}, \theta)$ is constructed from the solution of the Poisson equation (27b) by separation of variables, i.e., a particular solution can be found by assuming $\widetilde{\psi}_p(\widetilde{r}, \theta) = R(\widetilde{r})\, \Theta(\theta)$, so that for $f = R_f(\widetilde{r})\, \Theta_f(\theta)$ we get

$$\widetilde{r}^2 \frac{R_f(\widetilde{r})}{R(\widetilde{r})} \frac{\Theta_f(\theta)}{\Theta(\theta)} = \frac{\widetilde{r}}{R(\widetilde{r})} \frac{\mathrm{d}}{\mathrm{d}\widetilde{r}} \left(\widetilde{r} \frac{\mathrm{d}R}{\mathrm{d}\widetilde{r}}\right) + \frac{1}{\Theta} \frac{\mathrm{d}^2\Theta}{\mathrm{d}\theta^2}. \tag{B11}$$

Clearly, for separation of variables we require $\Theta''/\Theta = -\beta^2$ and $\Theta_f(\theta) = \Theta(\theta)$, which leads to the inhomogeneous Euler equation for $R(\widetilde{r})$:

$$\widetilde{r}^2 \frac{\mathrm{d}^2 R}{\mathrm{d}\widetilde{r}^2} + \widetilde{r} \frac{\mathrm{d}R}{\mathrm{d}\widetilde{r}} - \beta^2 R = \widetilde{r}^{\beta+2} R_f(\widetilde{r}), \;\; R_f = C_1\, \widetilde{r}^{2k}\, M\left(-\widetilde{r}^2/(2\varepsilon)\right), \tag{B12}$$

the solution of which can be constructed by variation of constants. Namely, let us look for a solution in the form $R(\widetilde{r}) = \widetilde{r}^{\beta+2} H(\zeta)$, so that it obeys

$$\zeta^2 H'' + (\beta + 3)\zeta H' + (\beta + 1)H = (C_1/4) M(\widehat{a}, \widehat{b}, \zeta). \tag{B13}$$

The homogenous part of this equation admits two linearly independent solutions, $h_1(\zeta) = \zeta^{-1}$ and $h_2(\zeta) = \zeta^{-(1+\beta)}$, so that a particular solution of the above equation can be sought in the form $H(\zeta) = A(\zeta)h_1 + B(\zeta)h_2$, which gives

$$H(\zeta) = \frac{C_1}{4\beta} \left[\zeta^{-1} \int_0^\zeta M(\widehat{a}, \widehat{b}, \widetilde{\zeta})\, \mathrm{d}\widetilde{\zeta} - \zeta^{-(1+\beta)} \int_0^\zeta \widetilde{\zeta}^{\beta}\, M(\widehat{a}, \widehat{b}, \widetilde{\zeta})\, \mathrm{d}\widetilde{\zeta}\right]. \tag{B14}$$

As a result, a general solution of the inhomogeneous part of the problem (27b) reads

$$\widetilde{\psi}_p(\widetilde{r}, \theta) = \sum_{m=0}^{\infty} (A_m \cos\beta_m\theta + B_m \sin\beta_m\theta)\, R_m(\widetilde{r}), \tag{B15}$$

where $R_m(\widetilde{r}) = \widetilde{r}^{\beta_m+2} H_m(\zeta)$ and $H_m(\zeta) = H(\zeta, \beta_m)$ correspond to the value $\beta_m = \beta_0 + m$, $\beta_0 = 1/2$.

The solution (B15) together with a general solution of the homogeneous (harmonic) part of the Poisson equation (27b) in polar coordinates,[75]

$$\widetilde{\psi}_h(\widetilde{r}, \theta) = \sum_{n=-\infty}^{+\infty} \widetilde{r}^{n+\frac{1}{2}} \left\{C_n \cos\left(n + \tfrac{1}{2}\right)\theta + D_n \sin\left(n + \tfrac{1}{2}\right)\theta\right\}, \tag{B16}$$

gives the solution uniformly valid in both viscous and inviscid regions:

$$\begin{aligned}\widetilde{\psi}(\widetilde{r}, \theta) = \widetilde{\psi}_p + \widetilde{\psi}_h = &\sum_{m=0}^{\infty} (A_m \cos\beta_m\theta + B_m \sin\beta_m\theta)\, R_m(\widetilde{r}) \\ &+ \sum_{n=-\infty}^{+\infty} \widetilde{r}^{n+\frac{1}{2}} \left\{C_n \cos\left(n + \tfrac{1}{2}\right)\theta + D_n \sin\left(n + \tfrac{1}{2}\right)\theta\right\}.\end{aligned} \tag{B17}$$

[1] A. A. Korobkin and V. V. Pukhnachov, "Initial stage of water impact," Annu. Rev. Fluid Mech. **20**, 159–185 (1988).
[2] A. A. Korobkin, *Impact of Liquid and Solid Masses* (Russian Academy of Sciences, Novosibirsk, 1997).

[3] N. E. Joukowsky, "On impact of two spheres, one of which being floating in liquid," Zap. Mat. Otd. Novorossiiskogo Obshchestva Estestvoispyt. **4**, 43–48 (1884).
[4] H. Rouse and I. Simon, *History of Hydraulics* (Dover Books, New York, 1963).
[5] T. H. von Karman, "The impact on seaplane floats during landing," Technical Report No. 321 (NACA, 1929).
[6] H. Wagner, "Über Stoss- und Gleitvorgänge an der Oberfläche von Flüssigkeiten," Z. Angew. Math. Mech. **12**, 193–215 (1932).
[7] L. I. Sedov, "On impact of a solid body floating on surface of incompressible liquid," Tr. Tsentr. Aerodin. Inst. **187**, 1–2 (1934).
[8] L. I. Sedov, *Two-Dimensional Problems of Hydrodynamics and Aerodynamics* (Interscience Publications, New York, 1965).
[9] G. R. G. Lewison, "On the reduction of slamming pressures," Trans. RINA **112**, 285–306 (1970).
[10] G. K. Kapsenberg, "Slamming of ships: where are we now?" Philos. Trans. R. Soc. A **369**, 2892–2919 (2011).
[11] T. Stevenson, *The Design and Construction of Harbours* (A. C. Black, Edinburgh, 1886).
[12] M. J. Cooker and D. H. Peregrine, "Pressure-impulse theory for liquid impact problems," J. Fluid Mech. **297**, 193–214 (1995).
[13] E. G. Richardson, "The impact of a solid on a liquid surface," Proc. Phys. Soc. **61**, 352–367 (1948).
[14] P. R. Garabedian, "Oblique water entry of a wedge," Commun. Pure Appl. Math. **6**, 157–165 (1953).
[15] S. T. Thoroddsen, "The ejecta sheet generated by the impact of a drop," J. Fluid Mech. **451**, 373–381 (2002).
[16] A. A. Korobkin, "Shallow-water impact problems," J. Eng. Math. **35**, 233–250 (1999).
[17] E. V. Ermanyuk and M. Ohkusu, "Impact of a disk on shallow water," J. Fluids Struct. **20**, 345–357 (2005).
[18] S. L. Chuang, "Experiments on flat-bottom slamming," J. Ship Res. **10**, 10–17 (1966).
[19] Y. L. Yakimov, "Influence of atmosphere at falling of bodies on water," Izv. Akad. Nauk SSSR, Mekh. Zhidk. Gaza **5**, 3–6 (1973).
[20] S. Gaudet, "Numerical simulation of circular disks entering the free surface of a fluid," Phys. Fluids **10**, 2489–2499 (1998).
[21] A. A. Korobkin, "Asymptotic theory of liquid-solid impact," Philos. Trans. R. Soc. London A **355**, 507–522 (1997).
[22] G. K. Batchelor, *An Introduction to Fluid Dynamics* (Cambridge University Press, Cambridge, 1967).
[23] M. A. Lavrentiev and B. V. Schabat, *Methoden der komplexen Funktionentheorie* (Deutscher Verlag der Wissenschaften, Berlin, 1967).
[24] L. A. Galin, "Impact of solid body on a compressible liquid surface," Prikl. Mat. Mekh. **11**, 547–550 (1947).
[25] T. F. Ogilvie, "Compressibility effects in ship slamming," Shiffstechnik **10**, 147–154 (1963).
[26] A. A. Korobkin, "Penetration of a blunt body into a slightly compressible liquid," J. Appl. Mech. Tech. Phys. **5**, 104–110 (1984).
[27] H. Lamb, *Hydrodynamics* (Cambridge University Press, New York, 1975).
[28] J. H. G. Verhagen, "Impact of a flat plate on a water surface," J. Ship Res. **11**, 211–223 (1967).
[29] S. K. Wilson, "A mathematical model for the initial stages of fluid impact in the presence of a cushioning fluid layer," J. Eng. Math. **25**, 265–285 (1991).
[30] L. G. Loitsyanskii, *Mechanics of Liquids and Gases* (Pergamon Press, New York, 1966).
[31] Kelvin's theorem is in general not applicable to suddenly accelerated fluid motion and, to the author's knowledge, has never been proven in such a form. However, particle image velocimetry measurements in the author's laboratory showed that the flow field for early times after the impact is essentially the same (within the experimental error) as predicted by the potential flow analysis. Following the standard proof of Kelvin's theorem,[41] with a little work to get around the product of generalized functions which brings them out of the linear space on which they are defined, one can identify the key conditions for Kelvin's theorem to be valid: (a) no formation of any discontinuity in the fluid body (cavitation) due to the impact and (b) the flow should be isentropic, which is usually not the case since entropy is known to grow as a shock wave propagates through the fluid.[41]
[32] A. Iafrati and A. A. Korobkin, "Initial stage of flat plate impact onto liquid free surface," Phys. Fluids **16**, 2214–2227 (2004).
[33] J. M. Oliver, "Water entry and related problems," Ph.D. thesis (University of Oxford, 2002).
[34] I. R. Peters, D. van der Meer, and J. M. Gordillo, "Splash wave and crown breakup after disc impact on a liquid surface," J. Fluid Mech. **724**, 553–580 (2013).
[35] A. Iafrati and A. A. Korobkin, "Hydrodynamic loads during early stage of flat plate impact onto water surface," Phys. Fluids **20**, 082104 (2008).
[36] A. Iafrati and A. A. Korobkin, "Asymptotic estimates of hydrodynamic loads in the early stage of water entry of a circular disk," J. Eng. Math. **69**, 199–224 (2011).
[37] R. Zhao, O. M. Faltinsen, and J. Aarnes, "Water entry of arbitrary two-dimensional sections with and without flow separation," in *Proceedings of the 21st International Symposium on Naval Hydrodynamics*, edited by E. Rood (National Academy Press, Trondheim, Norway, 1996), pp. 118–132.
[38] V. V. Sychev, A. I. Ruban, V. V. Sychev, and G. L. Korolev, *Asymptotic Theory of Separated Flows* (Cambridge University Press, New York, 1998).
[39] A. E. P. Veldman, "Boundary layer flow past a finite flat plate," Ph.D. thesis (Rijksuniversiteit Groningen, Holland, 1976).
[40] L. J. Clancy, *Aerodynamics* (Pitman Publishing Limited, London, 1975).
[41] L. D. Landau and E. M. Lifshitz, *Fluid Mechanics* (Pergamon, New York, 1987).
[42] One may perform further linearization of (12) by expanding u, v, and p about their values at $\theta = 0$, so for example the pressure term gives $\tilde{p}|_{\theta=h(t,r)} = \tilde{p}|_{\theta=0} + \tilde{p}_\theta|_{\theta=0} \cdot h(t,r) + \ldots$, which will be done in due course.
[43] Note that Yakimov[19] used the limit $l \to +\infty$, $V_0 \to 0$ such that $\alpha = V_0\sqrt{l}$ remains a finite non-zero constant, but such a limit is actually unnecessary, i.e., one can consider both V_0 and plate size l to be finite.
[44] Another "natural" choice of scaling $t \to \tau$, $(x, y) \to \alpha^{2/3} t^{2/3}(\tilde{x}, \tilde{y})$, $\mathbf{v} \to V_0\mathbf{v}$, $p \to \rho\alpha^{4/3} t^{-1/3}\tilde{p}$, makes the nonlinear terms of higher order, $O(\tau^{-2/3})$, compared to the time-derivative term and viscous terms still dominate with the effective Reynolds number $Re = \nu\alpha^{-4/3}\tau^{-4/3}$.

[45] An alternative way to appreciate the linear structure of (26) is first to realize that Eq. (1) is linear and due to continuity its extension to $t > 0$ must be linear too up to some finite time: thus one may assume that the Dirac delta-function $\delta_D(t)$ in the solution for the impact on an ideal fluid should be replaced by a delta-sequence $\delta_\varepsilon(t)$ in the impact on a real fluid, where ε represents the physical effect responsible for smoothening $\delta_D(t)$ such as viscosity ν. Under such an assumption one can estimate the terms in the NSEs as follows:

$$\underbrace{\frac{\partial \mathbf{v}}{\partial t}}_{V_0\sqrt{\frac{l}{r}}\delta_\varepsilon(t)} + \underbrace{(\mathbf{v}\cdot\nabla)\mathbf{v}}_{V_0^2\frac{l}{r^2}} = \underbrace{-\frac{1}{\rho}\nabla p}_{V_0\sqrt{\frac{l}{r}}\delta_\varepsilon(t)} + \underbrace{\nu\Delta\mathbf{v}}_{\nu V_0\sqrt{\frac{l}{r}}\frac{1}{r^2}} .$$

Viscous terms dominate over nonlinearity on the distances from the plate edge $r \le l Re_0^{-2}$, while viscous and nonlinear terms become important relative to the impulsive terms ($\mathbf{v}_t$ and $\nabla p/\rho$) on the distances

$$r \le \sqrt{\frac{\nu}{\delta_\varepsilon(t)}} \equiv r_\nu \text{ and } r \le \left(\frac{V_0^2 l}{\delta_\varepsilon^2(t)}\right)^{1/3} \equiv r_N = \left(\frac{r_\nu^4}{r_0}\right)^{1/3},$$

respectively, where r_ν is the distance where viscosity is of the same order as the impulsive terms and r_N the distance at which nonlinearity is of the same order as the impulsive terms. Since $r_N \sim \delta_\varepsilon^{-2/3}$ and $r_\nu \sim \delta_\varepsilon^{-1/2}$, there exists a time interval $[0, t^*)$ over which $r_N \ll r_\nu$ so that one needs to take viscosity into account but nonlinearity is contained to a smaller region in space, which qualitatively agrees with the results from (24). This means that the full nonlinear NSEs should be solved in this smaller region—the situation is analogous to the boundary layer flow around the trailing edge.[39] Same as in the latter problem, the presence of the full NSEs region, however, does not prevent from the construction of a solution elsewhere,[38] but is required to resolve the singularity completely. At some time r_N reaches r_ν and then first embraces the viscous region and eventually the inviscid one—thus, the "inviscid" studies,[32,34,35] which take into account the nonlinearity, apply for these later times.

[46] G. F. Carrier and C. C. Lin, "On the nature of the boundary layer near the leading edge of a flat plate," Q. Appl. Math. **6**, 63–68 (1948).

[47] A. I. van de Vooren and D. Dijkstra, "The Navier-Stokes solution for laminar flow past a semi-infinite flat plate," J. Eng. Math. **4**, 9–27 (1970).

[48] A. Yoshizawa, "Laminar viscous flow past a semi-infinite flat plate," J. Phys. Soc. Jpn. **28**, 776–779 (1970).

[49] K. Stewartson, "On the flow near the trailing edge of a flat plate," Proc. R. Soc. London A **306**, 275–290 (1968).

[50] A. F. Messiter, "Boundary-layer flow near the trailing edge of a flat plate," SIAM J. Appl. Math. **18**, 241–257 (1970).

[51] M. Abramowitz and I. A. Stegun, *Handbook of Mathematical Functions: with Formulas, Graphs, and Mathematical Tables* (Dover, New York, 1965).

[52] M. van Dyke, *Perturbation Methods in Fluid Mechanics* (Parabolic Press, Stanford, CA, 1975).

[53] H. K. Moffatt, "Viscous and resistive eddies near a sharp corner," J. Fluid Mech. **18**, 1–18 (1964).

[54] S. D. Howison, J. R. Ockendon, and J. M. Oliver, "Deep- and shallow-water slamming at small and zero deadrise angles," J. Eng. Math. **42**, 373–388 (2002).

[55] It is worth noting that Yakimov[19] came up with his scaling based on the analysis of the linear problem and verified self-similarity at the interface only. Yakimov's scaling (20) is effectively based on the assumption that $\mathbf{v} = \mathrm{d}\mathbf{r}/\mathrm{d}t$ together with the near-the-edge scaling (5) resulting from the complex variable solution (4). However, the formula $\mathbf{v} = \mathrm{d}\mathbf{r}/\mathrm{d}t$ is the equation for pathlines, i.e., the line traced by a given particle—this is a Lagrangian concept and therefore application of the deduced from it Yakimov's scaling to the equations in Eulerian variables is not appropriate. Such kind of an assumption can be valid only if the Lagrangian and Eulerian descriptions coincide, which are almost always different for unsteady problems—the streamlines and pathlines generally do not coincide in the unsteady case to which our problem belongs. At the interface, which is a material line, however, each point moves with the same velocity as the fluid thanks to the kinematic boundary condition (12c) and thus one arrives at the scaling (20), which explains why the comparison with experimental measurements of the interfacial motion[34] is in reasonable agreement with Yakimov's scaling.

[56] J. W. Glasheen and T. A. McMahon, "Vertical water entry of disks at low Froude numbers," Phys. Fluids **8**, 2078–2083 (1996).

[57] V. S. Vladimirov, *Equations of Mathematical Physics* (Mir, Moscow, 1984).

[58] The analytical solution constructed here is valid for short times when the plate displacement can be neglected as in the work by Iafrati and Korobkin.[32] The analysis of the problem when the plate displacement is taken into account seems to be more difficult as suggested in the follow-up work by the same authors,[35] which showed a spike in the pressure distribution near the plate edge. The latter is counter-intuitive as the pressure is expected to be at the maximum at the plate center and then monotonically diminish towards the plate edges as observed in the analogous problem of a plate traveling through fluid.[22] Noticing that the complex potential (4) changes to $f(z) = iV_0\left(z + ih - \sqrt{(z+ih)^2 - l^2}\right)$ for the plate traveling a distance $h = V_0 t$, one may see an origin of the singularity after Taylor expanding this expression near the plate edge for small h:

$$f(z) = iV_0\left(z - \sqrt{z^2 - l^2}\right) - V_0 h\left(1 - \frac{z}{\sqrt{z^2 - l^2}}\right) + \text{h.o.t.},$$

i.e., the origin of the higher order singularity compared to that in (4) is in the coordinate expansion which becomes invalid when $z = O(h)$.

[59] O. A. Ladyzhenskaya, *Mathematical Theory of Viscous Incompressible Flow* (Gordon and Breach, New York, 1969).

[60] G. I. Barenblatt, *Scaling, Self-Similarity, and Intermediate Asymptotics* (Cambridge University Press, New York, 1996).

[61] If one bases the analysis on Yakimov's scaling, then as argued by Iafrati and Korobkin[32] viscous effects in the vicinity of the plate edge can be neglected for early times if (using Yakimov's scaling) the effective Reynolds number $Re = Re_0^{-1}(V_0 t/l)^{-1/3} \ll 1$ with $Re_0 = V_0 l/\nu$ or, equivalently, for $t \gg (l/V_0)Re_0^{-3}$ (see also the discussion in Sec. IV). This inequality, in the argument of Iafrati and Korobkin,[32] is satisfied after the acoustic stage $V_0/(l/t) \gg V_0/c_0$, i.e., at the times longer than it takes for information to propagate over the distances of the order of the plate half-width l with sound speed c_0.

[62] C. Josserand and S. Zaleski, "Droplet splashing on a thin liquid film," Phys. Fluids **15**, 1650–1657 (2003).

[63] R. Krechetnikov and G. M. Homsy, "Crown-forming instability phenomena in the drop splash problem," J. Colloid Interface Sci. **331**, 555–559 (2009).

[64] R. Krechetnikov, "A linear stability theory on time-invariant and time-dependent spatial domains with symmetry: the drop splash problem," Dyn. PDE **8**, 47–67 (2011).

[65] R. Krechetnikov, "Rayleigh-Taylor and Richtmyer-Meshkov instabilities of flat and curved interfaces," J. Fluid Mech. **625**, 387–410 (2009).

[66] R. Krechetnikov, "Stability of liquid sheet edges," Phys. Fluids **22**, 092101 (2010).

[67] We call the flow near the plate the *wall jet* because it is how the inviscid flow field looks like with the maximum x-velocity near the plate as opposed to the standard boundary layer flow.

[68] This fact is also simple to understand from the following comparison of each term in the boundary layer momentum equation

$$\underbrace{\frac{\partial u}{\partial t}}_{V_0/t} + \underbrace{u\frac{\partial u}{\partial x} + u\frac{\partial u}{\partial y'}}_{V_0^2/l} = -\underbrace{\frac{1}{\rho}p_x}_{V_0/t} + \underbrace{\nu\frac{\partial^2 u}{\partial y'^2}}_{\nu V_0/\delta^2}.$$

The boundary layer is driven by the pressure gradient between the plate edge and the plate center, where it is initially determined by the pressure $p \sim \rho V_0 l/t$ and then drops to the steady-state stagnation pressure value $p \sim \rho V_0^2$ in time $t_s \sim l/V_0$ required to establish the flow. From the above comparison of the terms in the boundary layer equation, one can see that the nonlinearity is not important until t_s, when the boundary layer thickness δ reaches a steady state value $\sim \sqrt{\nu l/V_0}$. Note that while the boundary layer in our problem resembles the behavior of the standard Prandtl's boundary layer driven by a pressure gradient, it is also analogous to the wall jet since the velocity at infinity, $y \to -\infty$, decays to zero. However, in the standard wall jet[69,70] there is no driving pressure gradient and thus the scaling is different for the wall jet thickness δ and the time t_s to achieve a steady state:

$$\delta \sim c^{1/2}(\nu l)^{3/4},\ t_s \sim c\nu^{1/2}l^{3/2},$$

where $c = V_0^{-1/2}Q^{-1}$ is the constant dependent on the velocity V_0 and mass flux Q at the origin of the wall jet. It may seem counter-intuitive that t_s decreases with viscosity, but since the wall jet thickness decreases with viscosity faster than that of the boundary layer it takes less time to establish a solution for lower viscosity.

[69] M. B. Glauert, "The wall jet," J. Fluid Mech. **1**, 625–643 (1956).

[70] N. I. Akatnov, "Development of 2D laminar jet along a solid surface," Leningrad. Politekhn. Inst. Trudy **5**, 24–31 (1953).

[71] H. Schlichting and K. Gersten, *Boundary Layer Theory* (Springer-Verlag, New York, 2000).

[72] E. E. Kummer, "De integralibus quibusdam definitis et seriebus infinitis," J. Reine Angew. Math. **1837**(17), 228–242 (1837).

[73] Confluent hypergeometric functions were introduced by Kummer[72] and used, for example, to describe the behavior of charged particles in a Coulomb potential and thus naturally appear in the quantum mechanics of the hydrogen atom.

[74] J. Happel and H. Brenner, *Low Reynolds Number Hydrodynamics: with Special Applications to Particulate Media* (Prentice-Hall, Englewood Cliffs, NJ, 1965).

[75] A. N. Tikhonov and A. A. Samarskii, *Equations of Mathematical Physics* (Dover, New York, 2011).